Article

Phosphatase Specificity and Pathway Insulation in Signaling Networks

Michael A. Rowland,[1] Brian Harrison,[1] and Eric J. Deeds[1,2,3,*]
[1]Center for Computational Biology and [2]Department of Molecular Biosciences, University of Kansas, Lawrence, Kansas; and [3]Santa Fe Institute, Santa Fe, New Mexico

ABSTRACT Phosphatases play an important role in cellular signaling networks by regulating the phosphorylation state of proteins. Phosphatases are classically considered to be promiscuous, acting on tens to hundreds of different substrates. We recently demonstrated that a shared phosphatase can couple the responses of two proteins to incoming signals, even if those two substrates are from otherwise isolated areas of the network. This finding raises a potential paradox: if phosphatases are indeed highly promiscuous, how do cells insulate themselves against unwanted crosstalk? Here, we use mathematical models to explore three possible insulation mechanisms. One approach involves evolving phosphatase K_M values that are large enough to prevent saturation by the phosphatase's substrates. Although this is an effective method for generating isolation, the phosphatase becomes a highly inefficient enzyme, which prevents the system from achieving switch-like responses and can result in slow response kinetics. We also explore the idea that substrate degradation can serve as an effective phosphatase. Assuming that degradation is unsaturatable, this mechanism could insulate substrates from crosstalk, but it would also preclude ultrasensitive responses and would require very high substrate turnover to achieve rapid dephosphorylation kinetics. Finally, we show that adaptor subunits, such as those found on phosphatases like PP2A, can provide effective insulation against phosphatase crosstalk, but only if their binding to substrates is uncoupled from their binding to the catalytic core. Analysis of the interaction network of PP2A's adaptor domains reveals that although its adaptors may isolate subsets of targets from one another, there is still a strong potential for phosphatase crosstalk within those subsets. Understanding how phosphatase crosstalk and the insulation mechanisms described here impact the function and evolution of signaling networks represents a major challenge for experimental and computational systems biology.

INTRODUCTION

Signaling networks allow cells to sense changes in their environment and respond adaptively. One of the most common motifs in eukaryotic signaling networks consists of a kinase that phosphorylates another protein in the network. Phosphorylation often alters the function of the target protein; for instance, the target itself might be a kinase that only becomes active when it is phosphorylated. A second enzyme, called a phosphatase, generally catalyzes the removal of the phosphoryl group. Although they are generally less well studied than kinases, phosphatases play a crucial role in controlling the phosphorylation levels of target proteins and thus the response of signaling networks to external stimuli (1–3).

Metazoan signaling networks are often very complex, exhibiting a high degree of crosstalk where many enzymes are shared among multiple pathways (3–9). Crosstalk studies have generally concentrated on the interactions made by kinases, and the potential for phosphatases to contribute to signaling complexity has been largely overlooked (10). For instance, when developing mathematical models of signaling networks, and a phosphatase has not yet been identified for a particular phosphoprotein, investigators will often add an anonymous, independent, and often unsaturatable phosphatase to the model to fill in the gap (11–17). This approach obviously ignores any contribution that phosphatase-mediated crosstalk might make to the behavior of the network.

We recently used a set of mathematical models to explore whether phosphatases acting on multiple substrates could impact signaling dynamics. We found that the responses of substrates to incoming signals can be strongly coupled if they share a phosphatase (2). In particular, we considered a case in which two different substrate proteins in the network, S_1 and S_2, have two completely independent kinases but share a single phosphatase. In this case, signals that activate only one of the kinases can cause both substrates to respond in a switch-like manner. This occurs because the phosphorylated substrate (say S_2*) will act as a competitive inhibitor of the phosphatase, causing the other substrate to become active. This significantly increases S_1 phosphorylation even when the kinase specific to that substrate has very low activity.

Although more than 500 distinct kinases have been identified in the human genome, there are only ~150 phosphatases (18,19). Thus, there are not even enough phosphatases to assign a unique one to each kinase, let alone to each unique substrate in the network, as has commonly been assumed in modeling studies (11–17). In fact, it is well

Submitted July 25, 2014, and accepted for publication December 5, 2014.
*Correspondence: deeds@ku.edu
Editor: Dennis Bray.

0006-3495/15/02/0986/11 $2.00
http://dx.doi.org/10.1016/j.bpj.2014.12.011

established that phosphatases are often inherently promiscuous: well-characterized phosphatases have been shown to act on tens, if not hundreds, of substrates (20–22). This fact suggests a potential paradox: since by virtue of their relatively small numbers, each phosphatase must act on a large number of targets, it is unclear how the cell avoids rampant phosphatase-mediated crosstalk between distinct parts of the network (2).

In this work, we used mathematical models to investigate a variety of mechanisms that cells could deploy to prevent shared phosphatases from resulting in unwanted crosstalk. These models focus on a simplified scenario in which substrates share a single phosphatase but are otherwise unrelated (e.g., Fig. 1 *A*). Although this ignores crosstalk at the kinase level (2–9) and the fact that phosphatase activity is often itself regulated by the signaling network (23,24), it allows us to isolate a particular source of crosstalk and characterize various mechanisms the cell might use to prevent it.

Since phosphatases can only couple substrate responses if they are saturated (2), one natural approach to limiting the impact of the phosphatase crosstalk would be to evolve phosphatases with Michaelis constants (K_M) so large that they essentially cannot be saturated by their substrates. We showed that in this scenario, the substrates can no longer respond ultrasensitively to incoming signals, and the phosphatases become highly inefficient enzymes that must be expressed at high levels to ensure rapid substrate responses. A second mechanism that cells might employ involves disposing of specific phosphatases altogether and instead employing degradation of the substrate as a means of removing phosphorylated molecules from the system. This alternative approach to effective dephosphorylation would have the benefit of reducing the required number of targets per phosphatase, decreasing the potential for phosphatase coupling in the rest of the network. We found that this dephosphorylation mechanism also cannot generate ultrasensitive responses. Additionally, in order for degradation to yield rapid response kinetics, the phosphorylated substrate would have to be highly unstable, with half-lives on the order of tens of minutes, which would involve high energetic costs to the cell.

Phosphatase promiscuity is likely a larger problem for serine/threonine phosphatases than it is for tyrosine phosphatases (20,21,25–27). Interestingly, serine/threonine phosphatases such as PP2A often act as holoenzymes comprised of a catalytically active subunit, a scaffolding subunit, and an adaptor subunit that recruits specific substrates to the complex (20,27–33). Using our models, we demonstrated that these adaptor subunits can insulate signaling pathways from phosphatase crosstalk while still allowing each independent substrate to respond ultrasensitively. We found that the ability of adaptor subunits to insulate signals between different substrates depends upon the manner of adaptor binding. In particular, the adaptor must be able to bind the substrate independently of whether or not it is already bound in an active holoenzyme complex with the catalytic subunit. Focusing on the example of PP2A, it is likely that the substrate specificities of its adaptor subunits have evolved to functionally couple subsets of targets within the signaling network (20,27–33).

Overall, our work demonstrates that although certain mechanisms can allow cells to avoid widespread phosphatase crosstalk, each of these mechanisms involves a set of functional trade-offs that likely dictate which mechanism will evolve in any given situation. Although these mechanisms almost certainly reduce the overall level of crosstalk in the cell, our analysis of the PP2A example indicates that at least some phosphatase coupling likely remains. Characterizing the functional role of phosphatase-mediated

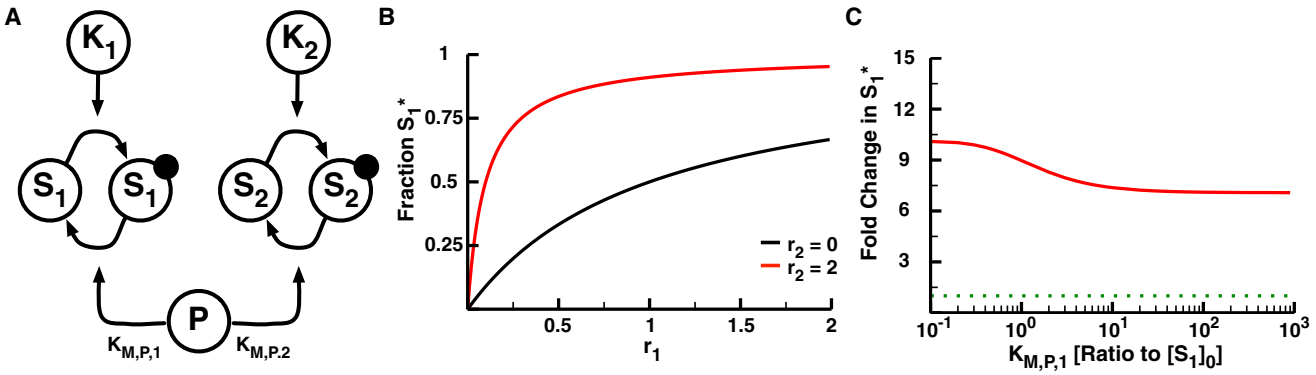

FIGURE 1 The 2-Kinase/1-Phosphatase loop. (*A*) Two independent kinases (K_1 and K_2) phosphorylate their respective substrates (S_1 and S_2). The solid circles indicate the phosphorylation of the substrates. A single shared phosphatase, *P*, dephosphorylates both substrates. (*B*) The fraction of phosphorylated S_1 (denoted as S_1*) as a function of response parameter r_1 when $r_2 = 0$ (*black*) and $r_2 = 2$ (*red*). r_1 and r_2 represent the ratio of the maximum velocity of the respective kinase to the maximum velocity of the phosphatase and are the dominant response parameters for the system. The initial concentrations of both S_1 and S_2 are set at 10 μM, $K_{M,P,1}$ at 1 mM, and $K_{M,P,2}$ at 1 μM. As such, S_1 does not saturate either the kinase K_1 or phosphatase, whereas S_2 saturates K_2 and *P*. Note the increase in phosphorylated S_1 in response to activation of the second loop, as described previously for this motif (2). (*C*) The fold change in S_1* as a function of $K_{M,P,1}$. The fold change in S_1* is calculated as the fraction S_1* at $r_2 = 2$ divided by the fraction S_1* at $r_2 = 0$. The dotted green line represents no change in S_1*. To see this figure in color, go online.

crosstalk in shaping network dynamics represents a major experimental and theoretical challenge in systems biology.

MATERIALS AND METHODS

Our models of 2-Kinase/1-Phosphatase dynamics, the corresponding systems of ordinary differential equations (ODEs), and details regarding the simulations are described in the Supporting Material. We used the CVODE library from SUNDIALS (34) to numerically integrate the systems of ODEs. The analytical solutions and subsequent derivations are also provided in the Supporting Material.

The half-lives of signaling proteins were taken from a published data set of the half-lives of proteins in mouse C2C12 cells (35). We analyzed the UniProt entry for each protein in this data set and checked for Gene Ontology (GO) annotations describing the protein as being a phosphoprotein. We also obtained the density curve for signaling protein half-lives using the default density estimator in R (36).

RESULTS

The promiscuity of phosphatases

As mentioned above, kinases vastly outnumber phosphatases in the human genome (18,19). To characterize the generality of this kinase/phosphatase mismatch across different species, we searched the UniProt database for ratios of kinases to phosphatases, and phosphoproteins to phosphatases (see Supporting Material for details) (37). We found that for most eukaryotes, there is no way to achieve a single, independent phosphatase per kinase, let alone substrate (as is often assumed, if implicitly, in modeling studies) (27). These findings are consistent with a variety of experimental studies in which phosphatases were shown to target tens to hundreds of phosphoproteins (20,21,25–27).

We previously demonstrated that phosphatases acting on multiple substrates could contribute to network crosstalk. Using a mathematical model in which a phosphatase is shared between two substrates with independent kinases (diagrammed in Fig. 1 *A*), one can show that the shared phosphatase couples the responses of the substrates so that the activation of one kinase increases the phosphorylation of both substrates through phosphatase inhibition (2). It is straightforward to derive the fraction of phosphorylated substrate S_1 at steady state for this system:

$$S_1^* = \frac{(r_1 - 1) - (K_{K,1} + r_1\alpha_{P,1}K_{P,1}) + \sqrt{((r_1 - 1) - (K_{K,1} + r_1\alpha_{P,1}K_{P,1}))^2 + 4(r_1 - 1)r_1\alpha_{P,1}K_{P,1}}}{2(r_1 - 1)}, \quad (1)$$

where $S_1^* \equiv [S_1^*]/[S_1]_0$ is the mole fraction of phosphorylated substrate S_1; $K_{K,1} \equiv K_{M,K,1}/[S_1]_0$ and $K_{P,1} \equiv K_{M,P,1}/[S_1]_0$ are the Michaelis constants of the substrate S_1 for the kinase K_1 and the shared phosphatase P divided by the total concentration of S_1; and $r_1 \equiv k_{cat,K,1}[K_1]_0/k_{cat,P,1}[P]_0$. Since protein concentrations remain constant over relevant timescales, r_1 serves as the response parameter that drives S_1 phosphorylation (2,38). The $\alpha_{P,1} \equiv 1 + [S_2^*]/K_{M,P,2}$ term represents the influence of S_2 on the phosphorylation of S_1. The solution for the fraction of phosphorylated S_2 at steady state is the same as Eq. 1 with different indices (e.g., $r_2 \equiv k_{cat,K,2}[K_2]_0/k_{cat,P,2}[P]_0$). Upon activation of the second loop (K_2-S_2), the phosphorylated S_2 acts as a competitive inhibitor of the phosphatase, increasing $\alpha_{P,1}$ if $[S_2^*]$ is large relative to $K_{M,P,2}$. This phosphatase inhibition results in an increase in S_1 phosphorylation (Fig. 1 *B*). The difference in S_1 phosphorylation due to K_2-S_2 activity can be illustrated as the fold change in S_1 phosphorylation upon K_2 stimulation, defined here as the concentration of phosphorylated S_1 at $r_2 = 2$ divided by the concentration of phosphorylated S_1 at $r_2 = 0$. Give this definition, we observe up to a 10-fold increase in phosphorylation of the first substrate at low values of r_1. Additionally, making P a poor phosphatase for S_1 by increasing $K_{M,P,1}$ does not remove the crosstalk, since $\alpha_{P,1}$ depends only on the saturation of the phosphatase by S_2^* (Fig. 1 *C*). Although the results in Fig. 1 focus on a case in which there is a single competing substrate S_2, multiple substrates can collectively saturate the phosphatase, leading to indirect activation of S_1 even when none of the competing substrates is at a high enough concentration to individually saturate the enzymes (see Supporting Material for details) (2).

The findings above indicate that on average, phosphatases are quite promiscuous, with tens to hundreds of substrates, and that this promiscuity can cause indirect activation of substrates due to phosphatase crosstalk (Fig. 1). In the following sections, we characterize a number of possible mechanisms that cells could use to minimize the impact of this crosstalk on the response of the network.

Removing coupling with unsaturatable phosphatases

Since phosphatase coupling is dependent upon the collective saturation of the phosphatase by its substrates, it follows that an unsaturatable phosphatase could insulate substrate responses. To investigate the effects of phosphatase saturation on crosstalk, we simultaneously increased both $K_{M,P,1}$ and $K_{M,P,2}$ in our 2-Kinase/1-Phosphatase model (Fig. 1 *A*). When the $K_{M,P}$ values are smaller than the total concentrations of the substrates, we see that the phosphorylation of S_1

at a low value of r_1 is increased ~10-fold upon activation of the second kinase. As the phosphatase K_M values are increased, however, the fold increase in S_1 phosphorylation drops until it reaches one, indicating that S_1 becomes insensitive to K_2 activity at $K_{M,P}$ values above ~10 times the total substrate concentration (Fig. 2 *A*).

The insulation provided by an unsaturated phosphatase comes at the cost of the loss of an ultrasensitive response of the substrates to incoming signal (2,39). The unsaturated phosphatase can no longer operate at its maximum velocity, and as such it takes very little active kinase to phosphorylate a significant fraction of S_1 at steady state (Fig. 2 *B*). One can understand these results by treating the system analytically. With an unsaturated phosphatase, the solution for the fraction of phosphorylated substrate becomes

$$S_1^* = \frac{(1+K_{K,1}+r_1K_{P,1}) - \sqrt{(1+K_{K,1}+r_1K_{P,1})^2 - 4r_1K_{P,1}}}{2}. \quad (2)$$

Note the lack of the α inhibition term from the shared phosphatase, since $K_{M,P,2} >> [S_2]_0$, $\alpha_{P,1} \approx 1$, resulting in a lack of phosphatase-mediated crosstalk. One can show that the analytical solution in Eq. 2 is strictly hyperbolic in r_1 regardless of the values of the kinetic parameters, confirming the lack of any possible ultrasensitive response (see Supporting Material for derivation) (39).

Another complication with an unsaturated phosphatase is the timescale on which it can dephosphorylate a pool of substrate molecules. To explore this issue, we initialized our system with a fully phosphorylated pool of S_1 molecules and no activity for the second kinase (i.e., $r_2 = 0$). This represents a pathway that has been fully activated by an incoming signal. We then ran this system with absolutely no kinase activity ($r_1 = 0$) to simulate the system after the removal of input. When $K_{M,P}$ is small, it takes <1 h to fully dephosphorylate all substrate. However, it takes longer as the phosphatase becomes unsaturated; for example, it takes >100 h to completely dephosphorylate the substrate when the $K_{M,P}$ is 100 times the total substrate concentration (Fig. 2 *C*). When $K_{M,P}$ is large, the time it takes to dephosphorylate half the substrates ($t_{1/2}$) follows

$$t_{1/2} = \frac{\log 2 \cdot K_{M,P,1}}{k_{cat,P}[P]_0}. \quad (3)$$

The dependence of $t_{1/2}$ on $K_{M,P,1}$ is thus linear, which can result in very long timescales when the enzyme becomes highly unsaturated. In cases where fast dephosphorylation of the substrate is important (say, in tightly controlling the duration of a cellular response, or when fast oscillations are necessary), the system can compensate for this increase in timescale by expressing more phosphatase (Fig. 2 *D*).

Interestingly, overexpression of the phosphatase alone can insulate substrate responses even when the K_M values are small, as long as the concentration of phosphatase becomes so high that the traditional Michaelis-Menten assumption that the enzymes are at much lower concentration than their substrates is broken (1). In this regime, however, the enzymes tend to sequester their substrates, reducing the concentration of unbound, phosphorylated

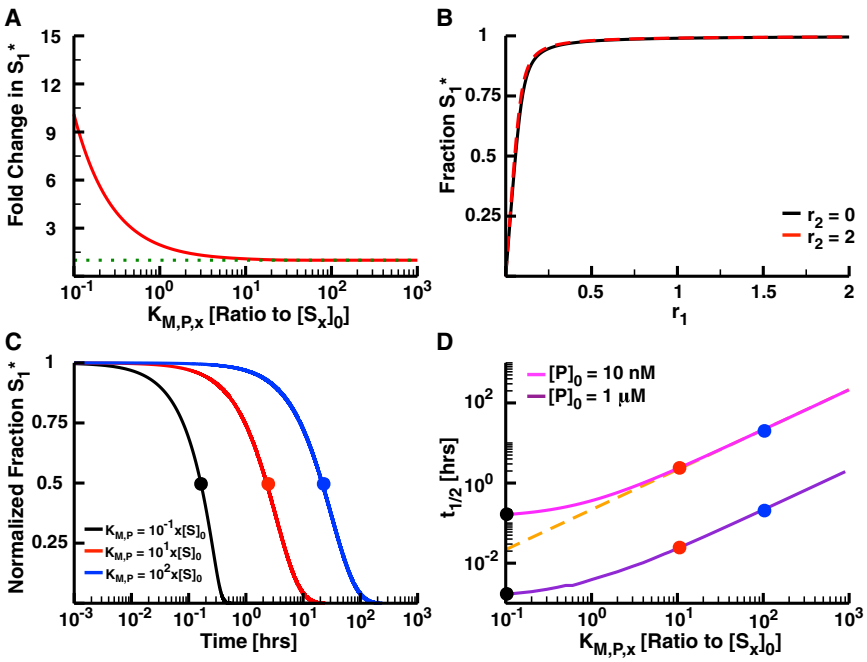

FIGURE 2 Removing coupling with unsaturatable phosphatases. (*A*) The fold increase in S_1 phosphorylation as a function of the $K_{M,P}$ of the shared phosphatase for both substrates in a 2-Kinase/1-Phosphatase loop. (*B*) The fraction S_1* as a function of r_1 at $r_2 = 0$ (*black*) and $r_2 = 2$ (*red*) when $K_{M,P} = 10\text{x}[S]_0$. Note that there is very little difference between these curves. (*C*) The normalized fraction of phosphorylated substrate S_1* as a function of time after the removal of input signal. In these simulations, the concentration of S_2 and K_2 are 0. The systems were allowed to run to steady state at high K_1 activity ($r_1 = 2$); at $t = 0$, the activity of the kinase was set to 0 (i.e., $r_1 = 0$). The y axes were normalized by $y_1 = (y - \min_y) / (\max_y - \min_y)$, where $\min_y$ is the fraction S_1* at $r_1 = 0$ and $\max_y$ is the fraction S_1* at $r_1 = 2$ at steady state. (*D*) The half-life of S_1 phosphorylation as a function of $K_{M,P}$ with two total concentrations of P (10 nM, *green*, and 1 μM, *purple*). Note that the black, red, and blue dots are shown to illustrate the relationship between (*D*) and (*C*). The dashed orange line shows the linear approximation of $t_{1/2}$ for highly unsaturated phosphatases ($t_{1/2} = K_{M,P}/k_{cat,P}[P]_0$). To see this figure in color, go online.

substrate available to participate in downstream reactions within the network (see Fig. S1). Thus, while phosphatase overexpression can result in insulation and reduce dephosphorylation timescales (Fig. 2 *D*), it can also reduce the capacity of the system to respond to incoming signals. As a result, many phosphatases (such as Msg5, which dephosphorylates the MAPK Fus3 in yeast) are at least an order of magnitude lower in concentration than their substrates (40,41).

An increased phosphatase K_M is the only mechanism cells could use to unsaturate the phosphatase. Previous experimental studies have demonstrated that binding of phosphorylated sites by SH-2 domain-containing or 14-3-3 proteins can shield the phosphoprotein from dephosphorylation, creating a reservoir phosphorylated substrate (42,43). The presence of such proteins would effectively reduce the concentration of substrate available to the phosphatase (and thus its saturation level) without influencing the saturation of the kinase. To consider the effects of this shielding phenomenon, we added substrate-specific reservoir proteins to our 2-Kinase/1-Phosphatase model. As expected, these reservoir proteins do insulate the substrates from crosstalk even when the K_M values are relatively small (see Fig. S2, A and B). However, since the phosphatase is effectively unsaturated, the substrates always respond hyperbolically to inputs. The dephosphorylation kinetics are also very slow in the presence of high concentrations of reservoir proteins, since the phosphatase must essentially wait for a substrate to be unbound long enough for it to bind and catalyze the dephosphorylation reaction (Fig. S2 C).

Thus, although unsaturating the phosphatase can insulate a substrate from the response of another substrate, this mechanism clearly involves a set of trade-offs. For one, none of the substrates can respond in a switch-like manner to incoming signals, so this mechanism cannot be deployed in cases where ultrasensitive responses are crucial (11,16,44–47). In addition, achieving fast dephosphorylation timescales may require high levels of phosphatase expression, which may become impractical (or limit the capacity of the system to respond at all) in cases where the K_M needed to achieve insulation is very large (Figs. 2 *D* and S1 A). These trade-offs likely limit the number of cases in which insulation via an unsaturated phosphatase represents an evolutionarily favored mechanism.

Degradation as a phosphatase substitute

The vast majority of work on modeling signal transduction has assumed that dephosphorylation occurs through the catalytic activity of a phosphatase (1,2,11–17). Although there are many clear cases in which phosphatases play this role, it is also possible for substrate degradation to serve as a dephosphorylation mechanism. The idea in this case is straightforward: phosphoproteins are synthesized in their unphosphorylated state, but both the unphosphorylated and phosphorylated states of the protein may be lost from the system due to degradation. When the total protein concentration (regardless of state) remains constant in time, the effect of synthesis and degradation effectively amounts to a first-order dephosphorylation term (see the Supporting Material for details). Substrates that rely on degradation as their phosphatase would not need a separate phosphatase enzyme, which would reduce the number of substrates upon which each phosphatase would have to act.

To characterize degradation as a phosphatase substitute, we built a mathematical model with a substrate responding to a single kinase without a phosphatase. In this model, we assume that the degradation process is completely unsaturatable. As a result, the degradation terms are all taken to be first order, and there is no degradation- or phosphatase-mediated crosstalk between pathways. In some cases, phosphorylation of a protein changes its half-life; for instance, the phosphorylated state of the protein may be less stable than the unphosphorylated state (48,49). To capture this possibility in our model, the unphosphorylated and phosphorylated substrates are degraded at different rates ($k_{deg,U}$ and $k_{deg,P}$ for the unphosphorylated and phosphorylate states, respectively). When the substrate is bound to a kinase, we assume that the kinase falls off the complex as the substrate is degraded. Unphosphorylated substrate is synthesized at a rate necessary to maintain a constant total substrate concentration at steady state (see Supporting Material for details). To parameterize the model, we obtained a range of half-lives by using UniProt to identify phosphoproteins from a published data set of protein half-lives in mouse C2C12 cells (35,37). Phosphoproteins in this data set have half-lives ranging from ~10 to 187 h, with a median of 31 h (Fig. 3 *A*). We used these values to set the range of biologically relevant degradation rates for the substrates.

We then ran this model to steady state using each of the phosphoprotein half-lives for a range of kinase concentrations. For these initial simulations, we assumed that the phosphorylation state does not influence the degradation rate (i.e., $k_{deg,U} = k_{deg,P}$). The response of the substrate to incoming signal is dependent on the half-life of the substrate (e.g., more stable phosphoproteins are more highly phosphorylated than less stable phosphoproteins; Fig. 3 *B*). However, substrates with any half-life in the mouse data set become completely phosphorylated when the kinase concentration is ≥ 1 nM, making these substrates highly sensitive to incoming signal. Note that the catalytic rate of the kinase in these simulations is 0.9 s^{-1}, which is close to the kinase catalytic rates that have been determined experimentally (50,51). Faster kinase catalytic rates would further reduce the kinase concentrations necessary to completely phosphorylate substrates with the observed half-lives.

To understand how the different degradation rates may affect substrate phosphorylation and sensitivity, we derived

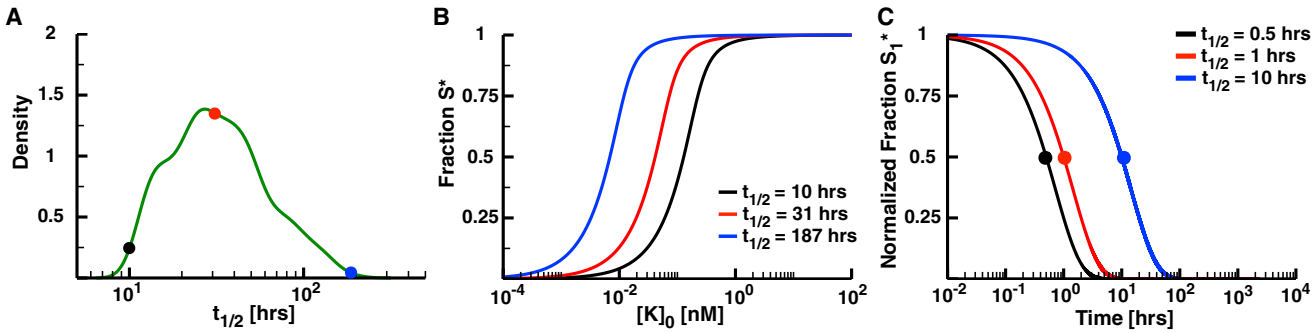

FIGURE 3 Degradation as a phosphatase. (*A*) The range of signaling protein half-lives in mouse C2C12 cells (35). The minimum reported half-life is 10 h (*black dot*), maximum is 187 h (*blue*), and median is 31 h (*red*). (*B*) The fraction S^* as a function of the concentration of active kinase, $[K]_0$. Note that the model for these panels includes only the kinase and degradable substrate. $[K]_0$ directly affects the parameter r_{deg}, which represents the ratio of the maximum velocity of the kinase to the maximum velocity of degradation ($k_{deg}\times[S]_0$). The value of r_{deg} will thus change for a constant concentration of kinase as the half-life changes. As such, any r_{deg} for a protein with a longer half-life will involve a lower concentration of kinase than that for a protein with a shorter half-life. (*C*) The normalized fraction S^* as a function of the time after setting kinase activity to 0 for substrates with half-lives of 0.5, 1, and 10 h. To see this figure in color, go online.

a solution for the fraction of phosphorylated S^* in this model:

$$S_1^* = \frac{\left(1 + r_{deg} + K_{deg}\right) - \sqrt{\left(1 + r_{deg} + K_{deg}\right)^2 - 4r_{deg}}}{2}, \tag{4}$$

where $r_{deg} \equiv k_{cat,K}[K]_0/k_{deg,P}[S]_0$ is the ratio of the maximum velocity of the kinase to the maximum velocity of substrate degradation. This solution includes a modified Michaelis constant $K_{M,deg} \equiv (k_{-,K} + k_{cat,K} + k_{deg,U})/k_{+,K}$, taking into account the degradation of the kinase-bound substrate, which is divided by the total substrate concentration to obtain K_{deg}. As expected based on our results for an unsaturatable phosphatase, one can show that the phosphorylation response of the substrate in this model can only be hyperbolic in r_{deg} (see Supporting Material for the derivation). As such, a signaling pathway that relies on degradation to remove phosphorylated substrate could never respond ultrasensitively to incoming signals.

Finally, the timescales required to degrade a pool of phosphorylated substrate based on the half-lives of phosphoproteins from the C2C12 data set would be very long. To demonstrate this, we ran the model at high levels of kinase activity ($r_{deg} = 2$) to steady state. We then set $r_{deg} = 0$ to simulate the system after removal of the input. Even with the shortest substrate half-life, the system requires ~100 h to completely dephosphorylate the substrate (Fig. 3 *C*). Complete dephosphorylation of the substrate in <1 h would require the phosphorylated state to have a half-life on the order of minutes. If the system needs to recover quickly from incoming signals, utilizing degradation as a phosphatase subunit would likely be quite inefficient, requiring a very unstable phosphorylated substrate. Maintaining a reasonable concentration of total substrate would in turn require a high rate of protein synthesis, resulting in a high energetic cost for the cell. Thus, although degradation could reduce the total substrate burden of phosphatases in the cell, it is likely to be employed only in cases where an ultrasensitive response is not necessary and when either slow dephosphorylation kinetics or the energetic costs of high protein turnover are functionally acceptable.

Role of phosphatase regulatory subunits in pathway isolation

Serine phosphatases such as PP1 and PP2A exist as holoenzymes: the catalytic subunit of PP2A binds to a scaffold subunit, which makes up the catalytic core. This core can then bind to one of many possible regulatory adaptor subunits, with each adaptor recruiting PP2A to a specific set of substrates (Fig. 4 *A*) (20,27–33). A previous study examined the mechanism of targeting of substrates by a regulatory subunit, as well as the effects of concentration and binding constants (52). However, that study did not consider whether regulatory subunits might provide insulation from phosphatase-mediated crosstalk. To investigate the role of these adaptors in isolating different pathways that share the same phosphatase catalytic core, we built two models, one ordered and one unordered, for binding of the phosphatase adaptor subunits. In the ordered model, the phosphatase catalytic core can bind two one of two adaptor subunits, creating two distinct holoenzymes. This holoenzyme can then specifically bind to and dephosphorylate a cognate substrate (diagrammed in the *inset* of Fig. 4 *B*). This model represents the standard case in which the holoenzyme first assembles and then acts on its substrates (30,33).

We first tested the ordered model to determine whether the interaction specificity of adaptor subunits is sufficient to isolate the responses of different substrates. To examine how the concentrations of the adaptor subunits affect substrate phosphorylation, we ran this model to steady state with a range of total adaptor concentrations (keeping the

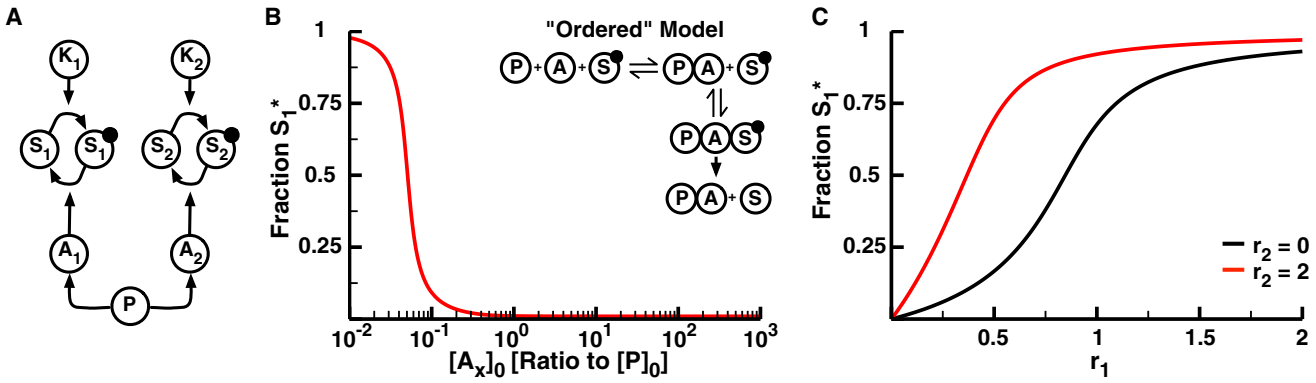

FIGURE 4 Ordered model of phosphatase regulatory adaptor subunits. (*A*) Diagram of the regulatory adaptor model. The previously described 2-Kinase/1-Phosphatase model (Fig. 1 *A*) was expanded to include two regulatory adaptor subunits, A_1 and A_2, that target the phosphatase to substrates S_1 and S_2, respectively. The phosphatase must bind an adaptor domain to bind and dephosphorylate either substrate. (*B*) The fraction S_1* as a function of the initial concentration of each adaptor subunit with low levels of K_1 activity ($r_1 = 0.05$) and high levels of K_2 activity ($r_2 = 2$). The concentrations of both adaptor subunits are equal and are varied simultaneously. Inset: Diagram of the ordered model. The phosphatase must first bind to an adaptor subunit. This complex can then bind to and dephosphorylate a phosphorylated substrate. (*C*) The fraction S_1* as a function of r_1 at $r_2 = 0$ (*black*) and $r_2 = 2$ (*red*) with $[A_x]_0 =$ 100 nM. In this model, the adaptor subunits do not eliminate the potential for phosphatase-mediated crosstalk even though they are perfectly specific for their respective substrates. To see this figure in color, go online.

concentrations of the two adaptors equivalent, i.e., $[A_1] = [A_2]$) and measured the fraction of phosphorylated S_1 at low levels of kinase 1 activation ($r_1 = 0.05$) and high levels of kinase 2 activity ($r_2 = 2$) (Fig. 4 *B*). In this model, a phosphatase can only act on its substrate when bound to an adaptor subunit. When the concentration of adaptors is less than that of the catalytic core, the total number of active phosphatases is thus limited by the adaptor concentration. As that concentration decreases, so does the concentration of active phosphatases, making the apparent value of *r* very high for both substrates and leading to an increase in S_1 phosphorylation (Fig. 4 *B*). Once the concentration of the adaptors exceeds that of the catalytic core, however, the concentration of the adaptors has little influence on S_1 phosphorylation (Fig. 4 *B*). At higher levels of kinase 1 activity, adaptor subunits provide no insulation between different substrates in this model: S_1 phosphorylation increases considerably as r_2 goes from 0 to 2 (Fig. 4 *C*). This indicates that although regulatory adaptor domains may help to target different phosphoproteins, their specificity cannot insulate substrates from phosphatase-mediated crosstalk in the ordered model. This is because the large pool of phosphorylated S_2 makes it far more likely that the holoenzyme will remain intact in order to bind and further dephosphorylate S_2. As such, the catalytic core is prevented from disassociating from its S_2-specific adaptor subunit and forming the holoenzyme specific to S_1, decreasing the concentration of phosphatase available to act on S_1.

The unordered model differs in that the adaptor subunit can bind its specific phosphoprotein without being bound to the catalytic core first. The adaptor-substrate dimer can then bind the catalytic core, resulting in substrate dephosphorylation (diagrammed in the *inset* of Fig. 5 *A*). This removes the ability of one substrate to sequester the catalytic core in the holoenzyme, since the core can dissociate from the regulatory adaptor subunit even in the presence of the phosphorylated substrate. At low concentrations of the adaptor subunits, the unordered model acts similarly to the ordered model (Fig. 5 *A*). However, as the adaptor concentration becomes very large, there is an increase in substrate phosphorylation. This is due to the prozone effect, i.e., as the concentration of adaptor increases, the system starts to produce many phosphatase-adaptor dimers and phosphorylated substrate-adaptor dimers. These dimers cannot bind to one another, which prevents the catalytic core from interacting with the substrate (41,52–57). Even though the prozone effect can influence the response at high adaptor concentrations, there is still a wide range of adaptor concentrations (>2 orders of magnitude) that provide robust phosphatase activity (Fig. 5 *A*). The unordered model also provides effective pathway insulation since there is essentially no change in S_1 phosphorylation as the second kinase switches between inactive and active ($r_2 = 0$ and $r_2 = 2$, respectively) (Fig. 5 *B*). Additionally, S_1 can respond ultrasensitively in r_1, although the apparent r_1 is about half of what is expected since the adaptor subunits split the available phosphatase between the two substrates.

PP2A is known to interact with a large number of substrates, yet only ~18 different regulatory subunits have been identified. To understand how this handful of subunits could allow the PP2A catalytic core to dephosphorylate so many substrates while maintaining a degree of pathway insulation, we built a network based on previously identified interactions between the regulatory subunits and the substrates of PP2A (Fig. 5 *C*) (20). This network depicts the interactions between 42 PP2A substrates and 18 regulatory subunits. Strikingly, only six of the substrates have interactions with more than one of the adaptors,

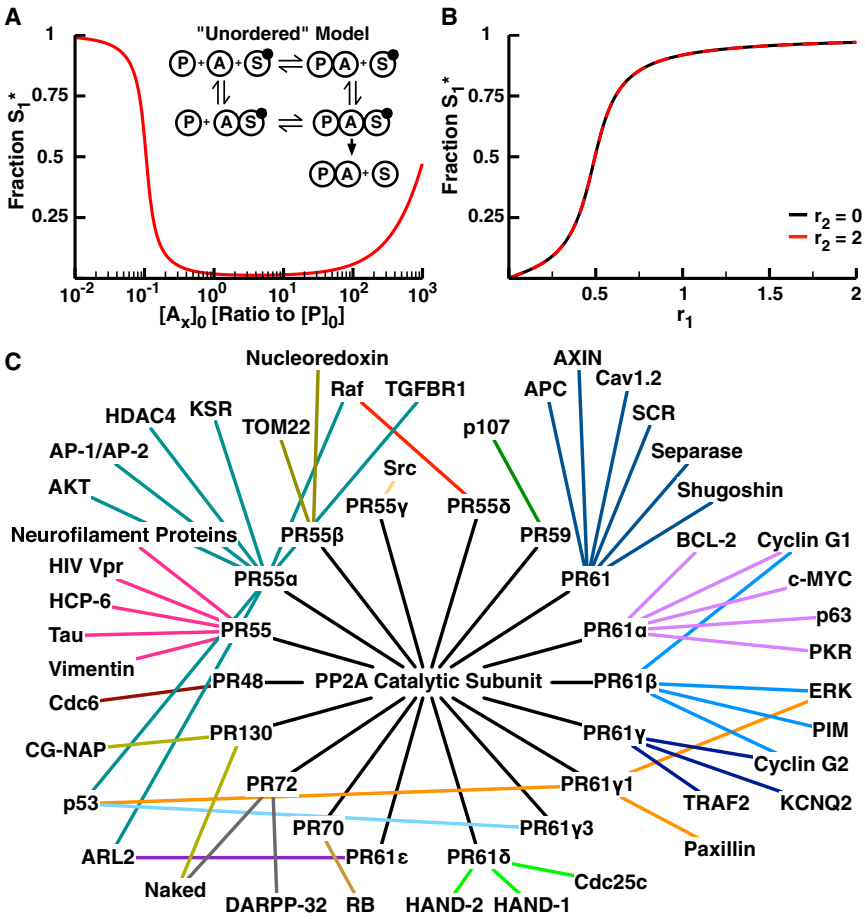

FIGURE 5 Unordered model of phosphatase regulatory adaptor subunits. (*A*) The fraction S_1* as a function of initial concentration of each adaptor subunit with low levels of K_1 activity ($r_1 = 0.05$) and high levels of K_2 activity ($r_2 = 2$). Inset: diagram of the unordered adaptor model. In this case, the adaptor subunit can bind to the substrate without previously binding to the phosphatase (*lower path*). (*B*) The fraction S_1* as a function of r_1 at $r_2 = 0$ (*black*) and $r_2 = 2$ (*red*) with $[A_x]_0 = 100$ nM. Note that this model provides insulation between the substrates. (*C*) Network diagram of the interactions of the PP2A catalytic subunit with each of 18 identified regulatory subunits (20). The PP2A holoenzyme formed by binding a regulatory subunit then interacts with a subset of the proteins in the network. To see this figure in color, go online.

and of these, only p53 interacts with three. The remaining substrates are all specific to a single regulatory subunit. According to our findings, these subsets of phosphoproteins would be insulated from one another, assuming the regulatory subunits can bind the phosphorylated substrates without binding the catalytic core. However, this insulation would not work within any given subset. Since they all share a single regulatory adaptor, the phosphoproteins in that subset would act as if they have a single, shared phosphatase. The coupling within groups of substrates could have positive phenotypic effects. For instance, PR55α interacts with AKT, AP-1/AP-2, HDAC4, and KSR, all of which are involved in the same signaling cascade (58–61). We previously showed that sharing a phosphatase among multiple members of the same signaling cascade increases the sensitivity of the cascade (2), so sharing the same PP2A holoenzyme within a subsection of a signaling network could increase its local responsiveness to external signals.

DISCUSSION

Although it is understood that both kinases and phosphatases act on a large number of targets, phosphatases have classically been considered to be more promiscuous than kinases. For example, although more than 20 phosphoproteins have been identified as substrates of the EGF/ErbB receptor tyrosine kinase (62), phosphatases such as PP2A dephosphorylate hundreds of substrates within the cell (20–22). Although the fact that phosphatases can be promiscuous has been appreciated for some time (20–22), it was only recently demonstrated that shared phosphatases can actually couple the responses of their substrates (2). Since phosphatases must act on large numbers of substrates, it is unclear how cells can ensure at least some degree of specificity in downstream responses to incoming signals. In this work, we extended our previous modeling efforts to consider three possible mechanisms whereby cells might insulate substrates from the possibility of phosphatase crosstalk. We found that each mechanism involves a set of unavoidable functional trade-offs that likely influence where and when they have evolved in eukaryotic signaling networks.

Perhaps the simplest mechanism would be to evolve phosphatases whose K_M values are so large that they cannot be saturated by their substrates. Although this mechanism is indeed effective in isolating the responses of substrates that share a particular phosphatase (Fig. 2, *A* and *B*), it

inherently creates phosphatases that are highly inefficient enzymes. As a result, the response of a substrate to upstream signals can no longer exhibit a switch-like, ultrasensitive character. Thus, it is unlikely that phosphatase inefficiency would be employed in cases where ultrasensitivity is a key component of the functional response (1,2,11,16,44–47). A second consequence of this inefficiency is slow dephosphorylation kinetics, which in turn means that high phosphatase expression levels are required before a particular substrate can quickly return to baseline activity levels after a signal is removed (Fig. 3, *C* and *D*). Other mechanisms that effectively desaturate the phosphatase, such as the expression of high levels of reservoir proteins that bind the phosphorylated state and prevent phosphatase binding, could also provide insulation but would have similar effects on the ultrasensitivity and dephosphorylation kinetics.

Protein degradation can also assume the role of an effective phosphatase, reducing the number of substrates that phosphatase enzymes might have to act upon in the cell. If we assume that degradation is both efficient and unsaturatable, then degradation can indeed prevent phosphatase crosstalk between substrates. As with the inefficient phosphatase mechanism, however, the lack of an ultrasensitive response and slow dephosphorylation kinetics might represent an issue for this particular mechanism in some cases. Even the least stable phosphoprotein in mouse cells would still require >100 h to return to baseline after removal of the signal (Fig. 3 *C*). Using degradation to fill the role of a phosphatase would thus require a very high (and very costly) rate of protein turnover in cases where fast response kinetics are necessary.

The final mechanism we considered here involved separate regulatory subunits recruiting a catalytic core to particular substrates. Although these subunits can clearly provide substrate specificity, it is not clear that they can actually insulate those substrates from one another. Indeed, if the phosphatase preassembles into a holoenzyme before interacting with the substrate (which is essentially the classical picture for this sort of enzyme (20,27–32)), even perfectly specific regulatory subunits cannot prevent phosphatase-mediated crosstalk (Fig. 4). If the regulatory subunits can bind their substrates independently of binding the catalytic core, however, this mechanism could provide insulation while still maintaining the possibility of an ultrasensitive response and fast dephosphorylation kinetics (Fig. 5). Deploying this mechanism, however, would require the evolution and expression of a distinct regulatory subunit for every set of phosphoproteins that the cell needs to isolate, which could represent a costly and evolutionarily complex solution to the problem of phosphatase coupling.

Our findings thus demonstrate that cells have a considerable degree of flexibility in the mechanisms they might use to insulate substrates from one another, despite the (relatively) small number of phosphatases in eukaryotic genomes. The question then arises: which of these mechanisms are deployed in any given situation, and to what extent are substrates truly isolated from one another? For instance, the well-characterized serine/threonine phosphatase PP2A acts as a holoenzyme with a regulatory subunit (20,27–32), and it is currently unclear whether the assembly of this holoenzyme follows the ordered or unordered model. Our results suggest that an experiment in which the adaptor concentration is increased (either directly in an in vitro setting or through overexpression in vivo) could establish which of these mechanisms is utilized by PP2A (Figs. 4 *B* and 5 *A*). Even if the assembly mechanism is unordered, PP2A-mediated crosstalk is still a strong possibility. Although the data presented in Fig. 5 *C* are certainly not complete (for instance, KSR and Akt share an additional regulatory subunit (63,64)), PP2A clearly does not have a distinct regulator for every substrate with which it interacts. Instead, these regulators have clearly evolved to interact with a specific subset of proteins, possibly coupling their responses in functionally meaningful ways (Fig. 5 *C*).

A major component of systems biology is the construction of formal mathematical or computational models of cellular regulatory systems, with the goal of understanding how cells process information from their environment and respond appropriately (65–68). In the case of complex eukaryotic signaling networks, a major barrier to this goal is the fact that dephosphorylation, whether by phosphatases or through some other mechanism, has been comparatively poorly characterized for most phosphoproteins in the network. The addition of anonymous and perfectly specific phosphatases to cover this gap may produce effective models of individual cascades or pathways (11–17), but it is unlikely that this practice will remain effective as larger, more genome-wide models of signaling networks are formulated. Experimentally determining the phosphatase structure of signaling systems and gaining a theoretical understanding of how that structure has evolved to generate and regulate crosstalk among pathways (Fig. 5 *C*) thus represents a major challenge for systems biology.

SUPPORTING MATERIAL

Supporting Materials and Methods and two figures are available at http://www.biophysj.org/biophysj/supplemental/S0006-3495(14)04755-9.

ACKNOWLEDGMENTS

The authors thank Walter Fontana, Vincent Danos, Christian Ray, Ryan Suderman, Carlos Lopez, James Faeder, and William Hlavacek for many interesting conversations regarding phosphatases in signaling networks.

REFERENCES

1. Goldbeter, A., and D. E. Koshland, Jr. 1981. An amplified sensitivity arising from covalent modification in biological systems. *Proc. Natl. Acad. Sci. USA.* 78:6840–6844.
2. Rowland, M. A., W. Fontana, and E. J. Deeds. 2012. Crosstalk and competition in signaling networks. *Biophys. J.* 103:2389–2398.
3. Junttila, M. R., S. P. Li, and J. Westermarck. 2008. Phosphatase-mediated crosstalk between MAPK signaling pathways in the regulation of cell survival. *FASEB J.* 22:954–965.
4. Danielpour, D., and K. Song. 2006. Cross-talk between IGF-I and TGF-β signaling pathways. *Cytokine Growth Factor Rev.* 17:59–74.
5. Hill, S. M. 1998. Receptor crosstalk: communication through cell signaling pathways. *Anat. Rec.* 253:42–48.
6. Javelaud, D., and A. Mauviel. 2005. Crosstalk mechanisms between the mitogen-activated protein kinase pathways and Smad signaling downstream of TGF-β: implications for carcinogenesis. *Oncogene.* 24:5742–5750.
7. Liu, Q., and P. A. Hofmann. 2004. Protein phosphatase 2A-mediated cross-talk between p38 MAPK and ERK in apoptosis of cardiac myocytes. *Am. J. Physiol. Heart Circ. Physiol.* 286:H2204–H2212.
8. Mayer, B. J., M. L. Blinov, and L. M. Loew. 2009. Molecular machines or pleiomorphic ensembles: signaling complexes revisited. *J. Biol.* 8:81.
9. Thomson, M., and J. Gunawardena. 2009. Unlimited multistability in multisite phosphorylation systems. *Nature.* 460:274–277.
10. Hunter, T. 2007. The age of crosstalk: phosphorylation, ubiquitination, and beyond. *Mol. Cell.* 28:730–738.
11. Huang, C. Y., and J. E. Ferrell, Jr. 1996. Ultrasensitivity in the mitogen-activated protein kinase cascade. *Proc. Natl. Acad. Sci. USA.* 93: 10078–10083.
12. Kholodenko, B. N. 2000. Negative feedback and ultrasensitivity can bring about oscillations in the mitogen-activated protein kinase cascades. *Eur. J. Biochem.* 267:1583–1588.
13. Shao, D., W. Zheng, …, C. Tang. 2006. Dynamic studies of scaffold-dependent mating pathway in yeast. *Biophys. J.* 91:3986–4001.
14. Kholodenko, B. N., O. V. Demin, …, J. B. Hoek. 1999. Quantification of short term signaling by the epidermal growth factor receptor. *J. Biol. Chem.* 274:30169–30181.
15. Schoeberl, B., C. Eichler-Jonsson, …, G. Müller. 2002. Computational modeling of the dynamics of the MAP kinase cascade activated by surface and internalized EGF receptors. *Nat. Biotechnol.* 20: 370–375.
16. Kim, S. Y., and J. E. Ferrell, Jr. 2007. Substrate competition as a source of ultrasensitivity in the inactivation of Wee1. *Cell.* 128:1133–1145.
17. Ahmed, S., K. G. Grant, …, J. M. Haugh. 2014. Data-driven modeling reconciles kinetics of ERK phosphorylation, localization, and activity states. *Mol. Syst. Biol.* 10:718.
18. Arena, S., S. Benvenuti, and A. Bardelli. 2005. Genetic analysis of the kinome and phosphatome in cancer. *Cell. Mol. Life Sci.* 62:2092–2099.
19. Manning, G., D. B. Whyte, …, S. Sudarsanam. 2002. The protein kinase complement of the human genome. *Science.* 298:1912–1934.
20. Eichhorn, P. J., M. P. Creyghton, and R. Bernards. 2009. Protein phosphatase 2A regulatory subunits and cancer. *Biochim. Biophys. Acta.* 1795:1–15.
21. Ren, L., X. Chen, …, D. Pei. 2011. Substrate specificity of protein tyrosine phosphatases 1B, RPTPα, SHP-1, and SHP-2. *Biochemistry.* 50:2339–2356.
22. Sacco, F., L. Perfetto, …, G. Cesareni. 2012. The human phosphatase interactome: An intricate family portrait. *FEBS Lett.* 586:2732–2739.
23. Porter, I. M., K. Schleicher, …, J. R. Swedlow. 2013. Bod1 regulates protein phosphatase 2A at mitotic kinetochores. *Nat. Commun.* 4:2677.
24. Araki, T., H. Nawa, and B. G. Neel. 2003. Tyrosyl phosphorylation of Shp2 is required for normal ERK activation in response to some, but not all, growth factors. *J. Biol. Chem.* 278:41677–41684.
25. Barua, D., J. R. Faeder, and J. M. Haugh. 2007. Structure-based kinetic models of modular signaling protein function: focus on Shp2. *Biophys. J.* 92:2290–2300.
26. Haugh, J. M., I. C. Schneider, and J. M. Lewis. 2004. On the cross-regulation of protein tyrosine phosphatases and receptor tyrosine kinases in intracellular signaling. *J. Theor. Biol.* 230:119–132.
27. Virshup, D. M., and S. Shenolikar. 2009. From promiscuity to precision: protein phosphatases get a makeover. *Mol. Cell.* 33:537–545.
28. Bollen, M. 2001. Combinatorial control of protein phosphatase-1. *Trends Biochem. Sci.* 26:426–431.
29. Goldberg, Y. 1999. Protein phosphatase 2A: who shall regulate the regulator? *Biochem. Pharmacol.* 57:321–328.
30. Sontag, E. 2001. Protein phosphatase 2A: the Trojan horse of cellular signaling. *Cell. Signal.* 13:7–16.
31. Virshup, D. M. 2000. Protein phosphatase 2A: a panoply of enzymes. *Curr. Opin. Cell Biol.* 12:180–185.
32. Xu, Y., Y. Xing, …, Y. Shi. 2006. Structure of the protein phosphatase 2A holoenzyme. *Cell.* 127:1239–1251.
33. Sontag, E., S. Fedorov, …, M. Mumby. 1993. The interaction of SV40 small tumor antigen with protein phosphatase 2A stimulates the map kinase pathway and induces cell proliferation. *Cell.* 75:887–897.
34. Hindmarsh, A. C., P. N. Brown, …, C. S. Woodward. 2005. SUNDIALS: suite of nonlinear and differential/algebraic equation solvers. *ACM Trans. Math. Softw.* 31:363–396.
35. Cambridge, S. B., F. Gnad, …, M. Mann. 2011. Systems-wide proteomic analysis in mammalian cells reveals conserved, functional protein turnover. *J. Proteome Res.* 10:5275–5284.
36. R Core Team 2013. R: A Language and Environment for Statistical Computing. R Foundation for Statistical Computing, Vienna, Austria.
37. Consortium, T. U.; UniProt Consortium 2013. Update on activities at the Universal Protein Resource (UniProt) in 2013. *Nucleic Acids Res.* 41:D43–D47.
38. Belle, A., A. Tanay, …, E. K. O'Shea. 2006. Quantification of protein half-lives in the budding yeast proteome. *Proc. Natl. Acad. Sci. USA.* 103:13004–13009.
39. Gomez-Uribe, C., G. C. Verghese, and L. A. Mirny. 2007. Operating regimes of signaling cycles: statics, dynamics, and noise filtering. *PLOS Comput. Biol.* 3:e246.
40. Ghaemmaghami, S., W. K. Huh, …, J. S. Weissman. 2003. Global analysis of protein expression in yeast. *Nature.* 425:737–741.
41. Suderman, R., and E. J. Deeds. 2013. Machines vs. ensembles: effective MAPK signaling through heterogeneous sets of protein complexes. *PLOS Comput. Biol.* 9:e1003278.
42. Rotin, D., B. Margolis, …, J. Schlessinger. 1992. SH2 domains prevent tyrosine dephosphorylation of the EGF receptor: identification of Tyr992 as the high-affinity binding site for SH2 domains of phospholipase C gamma. *EMBO J.* 11:559–567.
43. Chiang, C. W., G. Harris, …, E. Yang. 2001. Protein phosphatase 2A activates the proapoptotic function of BAD in interleukin- 3-dependent lymphoid cells by a mechanism requiring 14-3-3 dissociation. *Blood.* 97:1289–1297.
44. Bagowski, C. P., J. Besser, C. R. Frey, and J. E. Ferrell, Jr. 2003. The JNK cascade as a biochemical switch in mammalian cells: ultrasensitive and all-or-none responses. *Curr. Biol.* 13:315–320.
45. Hardie, D. G., I. P. Salt, …, S. P. Davies. 1999. AMP-activated protein kinase: an ultrasensitive system for monitoring cellular energy charge. *Biochem. J.* 338:717–722.
46. LaPorte, D. C., and D. E. Koshland, Jr. 1983. Phosphorylation of isocitrate dehydrogenase as a demonstration of enhanced sensitivity in covalent regulation. *Nature.* 305:286–290.

47. Meinke, M. H., J. S. Bishop, and R. D. Edstrom. 1986. Zero-order ultrasensitivity in the regulation of glycogen phosphorylase. *Proc. Natl. Acad. Sci. USA.* 83:2865–2868.

48. Pederson, T. M., D. L. Kramer, and C. M. Rondinone. 2001. Serine/threonine phosphorylation of IRS-1 triggers its degradation: possible regulation by tyrosine phosphorylation. *Diabetes.* 50:24–31.

49. Wang, Y., P. M. Nishina, and J. K. Naggert. 2009. Degradation of IRS1 leads to impaired glucose uptake in adipose tissue of the type 2 diabetes mouse model TALLYHO/Jng. *J. Endocrinol.* 203:65–74.

50. Lew, J., S. S. Taylor, and J. A. Adams. 1997. Identification of a partially rate-determining step in the catalytic mechanism of cAMP-dependent protein kinase: a transient kinetic study using stopped-flow fluorescence spectroscopy. *Biochemistry.* 36:6717–6724.

51. Grant, B. D., and J. A. Adams. 1996. Pre-steady-state kinetic analysis of cAMP-dependent protein kinase using rapid quench flow techniques. *Biochemistry.* 35:2022–2029.

52. Yang, J., and W. S. Hlavacek. 2011. Scaffold-mediated nucleation of protein signaling complexes: elementary principles. *Math. Biosci.* 232:164–173.

53. Oberdorf, R., and T. Kortemme. 2009. Complex topology rather than complex membership is a determinant of protein dosage sensitivity. *Mol. Syst. Biol.* 5:253.

54. Chapman, S. A., and A. R. Asthagiri. 2009. Quantitative effect of scaffold abundance on signal propagation. *Mol. Syst. Biol.* 5:313.

55. Levchenko, A., J. Bruck, and P. W. Sternberg. 2000. Scaffold proteins may biphasically affect the levels of mitogen-activated protein kinase signaling and reduce its threshold properties. *Proc. Natl. Acad. Sci. USA.* 97:5818–5823.

56. Bray, D., and S. Lay. 1997. Computer-based analysis of the binding steps in protein complex formation. *Proc. Natl. Acad. Sci. USA.* 94:13493–13498.

57. Douglass, Jr., E. F., C. J. Miller, …, D. A. Spiegel. 2013. A comprehensive mathematical model for three-body binding equilibria. *J. Am. Chem. Soc.* 135:6092–6099.

58. Gao, A., B. Liu, …, C. Huang. 2007. Phosphatidylinositol-3 kinase/Akt/p70S6K/AP-1 signaling pathway mediated benzo(a)pyrene-induced cell cycle alternation via cell cycle regulatory proteins in human embryo lung fibroblasts. *Toxicol. Lett.* 170:30–41.

59. Van Kanegan, M. J., and S. Strack. 2009. The protein phosphatase 2A regulatory subunits B′β and B′δ mediate sustained TrkA neurotrophin receptor autophosphorylation and neuronal differentiation. *Mol. Cell. Biol.* 29:662–674.

60. Zhang, W., B. J. Thompson, …, S. M. Cohen. 2011. MAPK/ERK signaling regulates insulin sensitivity to control glucose metabolism in Drosophila. *PLoS Genet.* 7:e1002429.

61. Vartanian, R., J. Masri, …, J. Gera. 2011. AP-1 regulates cyclin D1 and c-MYC transcription in an AKT-dependent manner in response to mTOR inhibition: role of AIP4/Itch-mediated JUNB degradation. *Mol. Cancer Res.* 9:115–130.

62. Kaushansky, A., A. Gordus, …, G. MacBeath. 2008. A quantitative study of the recruitment potential of all intracellular tyrosine residues on EGFR, FGFR1 and IGF1R. *Mol. Biosyst.* 4:643–653.

63. Cullis, J., D. Meiri, …, R. Rottapel. 2014. The RhoGEF GEF-H1 is required for oncogenic RAS signaling via KSR-1. *Cancer Cell.* 25:181–195.

64. Padmanabhan, S., A. Mukhopadhyay, …, H. A. Tissenbaum. 2009. A PP2A regulatory subunit regulates C. elegans insulin/IGF-1 signaling by modulating AKT-1 phosphorylation. *Cell.* 136:939–951.

65. Sorger, P. K. 2005. A reductionist's systems biology: opinion. *Curr. Opin. Cell Biol.* 17:9–11.

66. Chen, W. W., M. Niepel, and P. K. Sorger. 2010. Classic and contemporary approaches to modeling biochemical reactions. *Genes Dev.* 24:1861–1875.

67. Janes, K. A., and D. A. Lauffenburger. 2013. Models of signalling networks—what cell biologists can gain from them and give to them. *J. Cell Sci.* 126:1913–1921.

68. Chylek, L. A., L. A. Harris, …, W. S. Hlavacek. 2014. Rule-based modeling: a computational approach for studying biomolecular site dynamics in cell signaling systems. *Wiley Interdiscip. Rev. Syst. Biol. Med.* 6:13–36.

Phosphatase specificity and pathway insulation in signaling networks

Supporting Information

Michael A. Rowland[1], Brian Harrison[1], and Eric J. Deeds[1,2,3]

[1]Center for Bioinformatics, The University of Kansas, 2030 Becker Dr., Lawrence, KS 66047, USA
[2]Department of Molecular Biosciences, The University of Kansas, 2030 Becker Dr., Lawrence, KS 66047, USA
[3]Santa Fe Institute, 1399 Hyde Park Rd., Santa Fe, NM 87501, USA

Email: Eric Deeds - deeds@ku.edu;

Contents

1 Systems of Ordinary Differential Equations

1.1 2-Kinase/1-Phosphatase Loop with 2 Substrates

In order to characterize the effects of phosphatase saturation and competition on phosphatase-mediated crosstalk we used the 2-Kinase/1-Phosphatase Loop with 2 Substrates model that we have previously characterized [1]. The equations described below were derived and analyzed in our previous work; we include them here for completeness. The set of enzymatic reactions for the 2-Kinase/1-Phosphatase Loop with 2 Substrates model are:

$$K_1 + S_1 \underset{k_{-,K,1}}{\overset{k_{+,K,1}}{\rightleftharpoons}} K_1S_1 \xrightarrow{k_{cat,K,1}} K_1 + S_1^*$$

$$K_2 + S_2 \underset{k_{-,K,2}}{\overset{k_{+,K,2}}{\rightleftharpoons}} K_2S_2 \xrightarrow{k_{cat,K,2}} K_2 + S_2^*$$

$$P + S_1^* \underset{k_{-,P,1}}{\overset{k_{+,P,1}}{\rightleftharpoons}} PS_1^* \xrightarrow{k_{cat,P,1}} P + S_1$$

$$P + S_2^* \underset{k_{-,P,2}}{\overset{k_{+,P,2}}{\rightleftharpoons}} PS_2^* \xrightarrow{k_{cat,P,2}} P + S_2$$

Each contain three rates: the complex formation (k_+), the rate of complex dissociation (k_-), and catalytic rate (k_{cat}). These reactions are diagrammed in Fig. $2A$ of the main text. The set of ODEs describing the free enzymes are:

$$\frac{d[K_1]}{dt} = [K_1S_1]k_{-,K,1} + [K_1S_1]k_{cat,K,1} - [K_1][S_1]k_{+,K,1}$$
$$\frac{d[K_2]}{dt} = [K_2S_2]k_{-,K,2} + [K_2S_2]k_{cat,K,2} - [K_2][S_2]k_{+,K,2}$$
$$\frac{d[P]}{dt} = [PS_1^*]k_{-,P,1} + [PS_2^*]k_{-,P,2} + [PS_1^*]k_{cat,P,1} + [PS_2^*]k_{cat,P,2} - [P][S_1^*]k_{+,P,1} - [P][S_2^*]k_{+,P,2}$$

The set of ODEs describing the free unphosphorylated substrates are:

$$\frac{d[S_1]}{dt} = [K_1S_1]k_{-,K,1} + [PS_1^*]k_{cat,P,1} - [K_1][S_1]k_{+,K,1}$$
$$\frac{d[S_2]}{dt} = [K_2S_2]k_{-,K,2} + [PS_2^*]k_{cat,P,2} - [K_2][S_2]k_{+,K,2}$$

The set of ODEs describing the free phosphorylated substrates are:

$$\frac{d[S_1^*]}{dt} = [PS_1^*]k_{-,P,1} + [K_1S_1]k_{cat,K,1} - [P][S_1^*]k_{+,P,1}$$
$$\frac{d[S_2^*]}{dt} = [PS_2^*]k_{-,P,2} + [K_2S_2]k_{cat,K,2} - [P][S_2^*]k_{+,P,2}$$

The set of ODEs describing the enzyme-substrate complexes are:

$$\frac{d[K_1S_1]}{dt} = [K_1][S_1]k_{+,K,1} - [K_1S_1]k_{-,K,1} - [K_1S_1]k_{cat,K,1}$$
$$\frac{d[K_2S_2]}{dt} = [K_2][S_2]k_{+,K,2} - [K_2S_2]k_{-,K,2} - [K_2S_2]k_{cat,K,2}$$
$$\frac{d[PS_1^*]}{dt} = [P][S_1^*]k_{+,P,1} - [PS_1^*]k_{-,P,1} - [PS_1^*]k_{cat,P,1}$$
$$\frac{d[PS_2^*]}{dt} = [P][S_2^*]k_{+,P,2} - [PS_2^*]k_{-,P,2} - [PS_2^*]k_{cat,P,2}$$

For purposes of display we used the following rate parameters:

Parameter	Value
$k_{+,K,i}$	0.001 $\text{nM}^{-1}\text{s}^{-1}$
$k_{-,K,i}$	0.1-999.1 s^{-1}
$k_{cat,K,i}$	0.9 s^{-1}
$k_{+,P,i}$	0.001 $\text{nM}^{-1}\text{s}^{-1}$
$k_{-,P,i}$	0.1-999.1 s^{-1}
$k_{cat,P,i}$	0.9 s^{-1}

where $i = 1$ or 2. The ranges listed for the dissociation rates (i.e. $k_{-,K,i}$) are used to set the K_M's of the enzymes in different simulations. Note that, while the values of these parameters are not meant to describe any specific enzyme, they are within the range of values obtained for kinases and phosphatases experimentally [2–4].

We used the following initial conditions for all of our simulations:

Molecular Species	Initial Concentration
K_1	0-20 nM
K_2	0-20 nM
P	10 nM-1mM
S_1	10 μM
S_2	0,10 μM

with the remaining molecular species having initial concentrations of 0. The ranges of concentrations of K_1 and K_2 are used to vary the values of r_1 and r_2.

This model was used to generate Fig. 1*B* and *C* of the main text. The concentration of K_2 was set to 0 for $r_2 = 0$ and to 20 nM for $r_2 = 2$. The concentration of K_1 was set between 0-20 nM to vary r_1 between 0 and 2. Both substrates are present at a concentration of 10μM. The values of $k_{-,K,1}$ and $k_{-,P,1}$ were both set to 999.1 s^{-1} so that $K_{M,K,1} = K_{M,P,1} = 100 \times [S_1]_0$, while $k_{-,K,2}$ and $k_{-,P,2}$ were set to 0.1 s^{-1} so that $K_{M,P,2} = K_{M,K,2} = 100 \times [S_2]_0$.

We also used this model to generate Fig. 2 of the main text. In Fig. 2*A*, $K_{M,P,i}$ was set by changing the values of $k_{-,P,1}$ and $k_{-,P,2}$ between 0.1-999.1 s^{-1}. The value of r_1 was set in Fig. 2*B* by setting the concentration of K_1 between 0-20 nM, and the concentration of K_2 was set to 0 for

$r_2 = 0$ and to 20 nM for $r_2 = 2$. For Fig. 2*C*, we first ran the model with $K_2 = S_2 = 0$ to steady state with the initial concentration of K_1 at 20 nM ($r_1 = 2$). We then removed all K_1 molecules from the system. The bound S_1 was added back to the concentration of unphosphorylated S_1. The simulations were then resumed to obtain the time courses visualized in Fig. 2*C*. $K_{M,P}$ was set by using values of $k_{-,P,2,1} = 0.1$ s^{-1}, 9.1 s^{-1}, and 99.1 s^{-1}. The fraction of phosphorylated S_1^* was normalized so that $\hat{S}_1^*(t) = (max(S_1^*) - S_1^*(t))/(max(S_1^*) - min(S_1^*))$. Fig. 2*D* was obtained using the same procedures as in Fig. 3*C*, setting $K_{M,P}$ by using values of $k_{-,P,2,1} = 0.1$-999.1 s^{-1}. The half-time of S_1^* phosphorylation was obtained by finding the time $t_{1/2} = t$ where $\hat{S}_1^*(t) = 0.5$. The total concentration of the phosphatase was set to either 10 nM (magenta curve), or 1 μM (purple curve).

To test the effectiveness of an increased phosphatase concentration in insulating substrates against phosphatase crosstalk while maintaining strong $K_{M,P,i}$ values, we set $K_{M,P,i} = 1\mu$M, $r_1 = 0.05$, $r_2 = 2$ and varied the concentration of the phosphatase from 10 nM to 1 mM (Fig. S1).

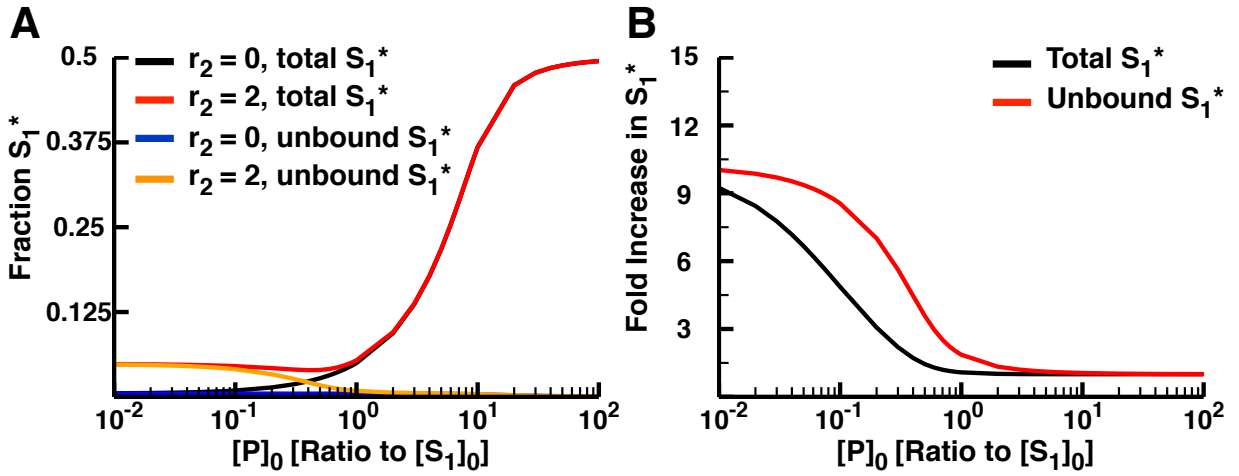

Figure S1: The effects of increased phosphatase concentration on substrate crosstalk with strong $K_{M,P,i}$s (*A*) The fraction S_1^* as a function of the concentration of the phosphatase. The concentration of the kinase is increased in order to maintain the values of r_1 and r_2 with constant catalytic rates for different concentrations of the phosphatase. At low concentrations of P, S_1 phosphorylation is increased by activation of the S_2 pathway, moving from $r_2 = 0$ (black) to $r_2 = 2$ (red). As P is expressed in concentrations greater than the substrates, the difference between the curves is removed. However, the fraction S_1^* is greatly increased. Additionally, the fraction of unbound S_1^* decreases with $[P]_0$, indicating that the increase in total fraction S_1^* is likely due to it being bound to the phosphatase. (*B*) The fold increase in S_1^* as a function of the concentration of the phosphatase. As stated above, the crosstalk between S_1 and S_2 is removed when the phosphatase is present in concentrations larger than those of the substrates.

1.2 2-Kinase/1-Phosphatase Loop with 2 Substrates and 2 Reservoir Proteins

In order to characterize the effects of reservoir proteins that bind to and shield phosphorylated substrates from dephosphorylated on phosphatase-mediated crosstalk we expanded the 2-Kinase/1-Phosphatase Loop with 2 Substrates model to include two substrate-specific reservoir

proteins, R_1 and R_2. The set of enzymatic reactions for the model are:

$$K_1 + S_1 \underset{k_{-,K,1}}{\overset{k_{+,K,1}}{\rightleftharpoons}} K_1S_1 \xrightarrow{k_{cat,K,1}} K_1 + S_1^*$$

$$K_2 + S_2 \underset{k_{-,K,2}}{\overset{k_{+,K,2}}{\rightleftharpoons}} K_2S_2 \xrightarrow{k_{cat,K,2}} K_2 + S_2^*$$

$$P + S_1^* \underset{k_{-,P,1}}{\overset{k_{+,P,1}}{\rightleftharpoons}} PS_1^* \xrightarrow{k_{cat,P,1}} P + S_1$$

$$P + S_2^* \underset{k_{-,P,2}}{\overset{k_{+,P,2}}{\rightleftharpoons}} PS_2^* \xrightarrow{k_{cat,P,2}} P + S_2$$

$$R_1 + S_1^* \underset{k_{-,R,1}}{\overset{k_{+,R,1}}{\rightleftharpoons}} R_1S_1^*$$

$$R_2 + S_2^* \underset{k_{-,R,2}}{\overset{k_{+,R,2}}{\rightleftharpoons}} R_2S_2^*$$

The set of ODEs describing the free enzymes are:

$$\frac{d[K_1]}{dt} = [K_1S_1]k_{-,K,1} + [K_1S_1]k_{cat,K,1} - [K_1][S_1]k_{+,K,1}$$
$$\frac{d[K_2]}{dt} = [K_2S_2]k_{-,K,2} + [K_2S_2]k_{cat,K,2} - [K_2][S_2]k_{+,K,2}$$
$$\frac{d[P]}{dt} = [PS_1^*]k_{-,P,1} + [PS_2^*]k_{-,P,2} + [PS_1^*]k_{cat,P,1} + [PS_2^*]k_{cat,P,2} - [P][S_1^*]k_{+,P,1} - [P][S_2^*]k_{+,P,2}$$

The set of ODEs describing the free unphosphorylated substrates are:

$$\frac{d[S_1]}{dt} = [K_1S_1]k_{-,K,1} + [PS_1^*]k_{cat,P,1} - [K_1][S_1]k_{+,K,1}$$
$$\frac{d[S_2]}{dt} = [K_2S_2]k_{-,K,2} + [PS_2^*]k_{cat,P,2} - [K_2][S_2]k_{+,K,2}$$

The set of ODEs describing the free phosphorylated substrates are:

$$\frac{d[S_1^*]}{dt} = [PS_1^*]k_{-,P,1} + [K_1S_1]k_{cat,K,1} + [R_1S_1^*]k_{-,R,1} - [P][S_1^*]k_{+,P,1} - [R_1][S_1^*]k_{+,R,1}$$
$$\frac{d[S_2^*]}{dt} = [PS_2^*]k_{-,P,2} + [K_2S_2]k_{cat,K,2} + [R_2S_2^*]k_{-,R,2} - [P][S_2^*]k_{+,P,2} - [R_2][S_2^*]k_{+,R,2}$$

The set of ODEs describing the enzyme-substrate complexes are:

$$\frac{d[K_1S_1]}{dt} = [K_1][S_1]k_{+,K,1} - [K_1S_1]k_{-,K,1} - [K_1S_1]k_{cat,K,1}$$
$$\frac{d[K_2S_2]}{dt} = [K_2][S_2]k_{+,K,2} - [K_2S_2]k_{-,K,2} - [K_2S_2]k_{cat,K,2}$$
$$\frac{d[PS_1^*]}{dt} = [P][S_1^*]k_{+,P,1} - [PS_1^*]k_{-,P,1} - [PS_1^*]k_{cat,P,1}$$
$$\frac{d[PS_2^*]}{dt} = [P][S_2^*]k_{+,P,2} - [PS_2^*]k_{-,P,2} - [PS_2^*]k_{cat,P,2}$$

The set of ODEs describing the free reservoir proteins are:

$$\frac{d[R_1]}{dt} = [R_1S_1^*]k_{-,R,1} - [R_1][S_1^*]k_{+,R,1}$$
$$\frac{d[R_2]}{dt} = [R_2S_2^*]k_{-,R,2} - [R_2][S_2^*]k_{+,R,2}$$

The set of ODEs describing the reservoir-substrate complexes are:

$$\frac{d[R_1S_1^*]}{dt} = [R_1][S_1^*]k_{+,R,1} - [R_1S_1^*]k_{-,R,1}$$
$$\frac{d[R_2S_2^*]}{dt} = [R_2][S_2^*]k_{+,R,2} - [R_2S_2^*]k_{-,R,2}$$

For purposes of display we used the following rate parameters:

Parameter	Value
$k_{+,K,i}$	0.001 $\text{nM}^{-1}\text{s}^{-1}$
$k_{-,K,i}$	0.1-999.1 s^{-1}
$k_{cat,K,i}$	0.9 s^{-1}
$k_{+,P,i}$	0.001 $\text{nM}^{-1}\text{s}^{-1}$
$k_{-,P,i}$	0.1-999.1 s^{-1}
$k_{cat,P,i}$	0.9 s^{-1}
$k_{+,R,i}$	0.001 $\text{nM}^{-1}\text{s}^{-1}$
$k_{-,R,i}$	0.01 s^{-1}

where $i = 1$ or 2. The ranges listed for the dissociation rates (i.e. $k_{-,K,i}$) are used to set the K_M's of the enzymes in different simulations. Note that, while the values of these parameters are not meant to describe any specific enzyme, they are within the range of values obtained for kinases and phosphatases experimentally [2–4].

We used the following initial conditions for all of our simulations:

Molecular Species	Initial Concentration
K_1	0-20 nM
K_2	0-20 nM
P	10 nM, 1μM
S_1	10 μM
S_2	0,10 μM
R_1	0-100 μM
R_2	0-100 μM

with the remaining molecular species having initial concentrations of 0. The ranges of concentrations of K_1 and K_2 are used to vary the values of r_1 and r_2.

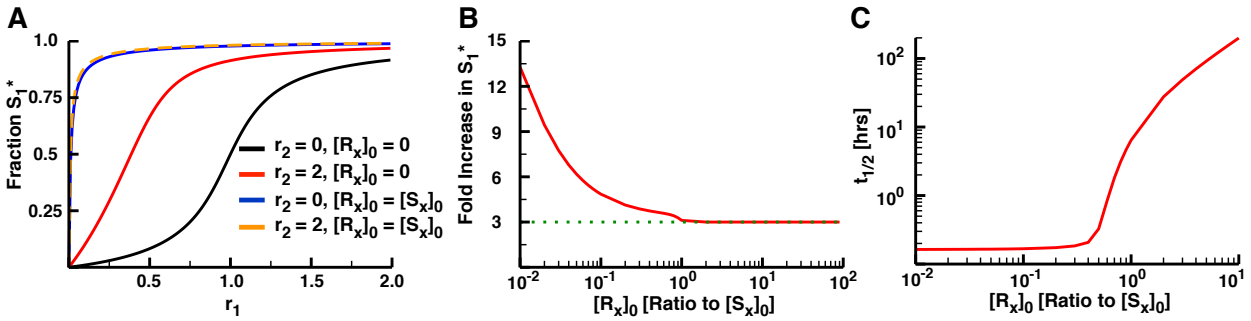

Figure S2: The effects of reservoir proteins on substrate crosstalk (A) The fraction S_1^* as a function of r_1. Without the reservoir proteins, S_1 responds to signals from S_2 (red versus black curves). The crosstalk is removed with the addition of the reservoir proteins (orange versus blue curves). Note, however, that the response becomes hyperbolic in r_1. (B) The fold increase in S_1^* as a function of reservoir protein concentration. As the concentrations of the reservoir proteins increases, the crosstalk between the substrates is gradually removed. (C) The half-life of S_1 phosphorylation as a function of the concentration of reservoir proteins. Note that when the reservoir proteins are at stoichiometric or greater concentrations, the time required to completely dephosphorylate the substrates greatly increases.

1.3 2-Kinase/1-Phosphatase Loop with Many Substrates

The expression for the fraction of phosphorylation S_1^* in a 2K1P loop in which kinase K_2 and P act upon N substrates is similar to the expression for a 2K1P loop with 2 substrates we have previously derived (equation 1 in the main text) [1]. The only difference in this case is the value of $\alpha_{P,1}$, the inhibitory term that captures the effects of the competing substrates on the phosphatase. In a model with N substrates, this term becomes:

$$\alpha_{P,1} = 1 + \sum_{i \neq 1} \frac{[S_i^*]}{K_{M,P,i}} \tag{1.1}$$

Note that the value of $\alpha_{P,1}$, and thus the inhibition of the phosphatase, depends on the total saturation of the phosphatase across all its substrates. A set of substrates that all respond to the same signal can thus cause phosphatase crosstalk with other proteins in the network, even if none of those substrates is at high enough concentration to saturate the phosphatase individually.

1.4 1-Kinase/1-Substrate Model with Synthesis and Degradation

In order to characterize the effectiveness of synthesis and degradation of a substrate as a replacement for the phosphatase, we created the 1-Kinase/1-Substrate model with Synthesis and Degradation. The set of enzymatic reactions for this system are:

$$K + S \underset{k_-}{\overset{k_+}{\rightleftharpoons}} KS \xrightarrow{k_{cat}} K + S^*$$

$$S \xrightarrow{k_{deg,U}} \emptyset$$
$$KS \xrightarrow{k_{deg,U}} K$$
$$S^* \xrightarrow{k_{deg,P}} \emptyset$$
$$\emptyset \xrightarrow{k_{synth}} S$$

where $k_{deg,U}$ and $k_{deg,P}$ are the degradation rates of unphosphorylated and phosphorylated S. This model includes separate degradation rates for the unphosphorylated and phosphorylated substrate ($k_{deg,U}$ and $k_{deg,P}$), since phosphorylation of the substrate might either increase or decrease the stability of the protein. The ODE describing the free kinase is:

$$\frac{d[K]}{dt} = [KS]k_- + [KS]k_{cat} + [KS]k_{deg,U} - [K][S]k_+$$

The ODE describing the free unphosphorylated substrate is:

$$\frac{d[S]}{dt} = [KS]k_- + k_{synth} - [K][S]k_+ - [S]k_{deg,U} \tag{1.2}$$

The ODE describing the free phosphorylated substrate is:

$$\frac{d[S^*]}{dt} = [KS]k_{cat} - [S^*]k_{deg,P}$$

The ODE describing the concentration of kinase-substrate complex is:

$$\frac{d[KS]}{dt} = [K][S]k_+ - [KS]k_- - [KS]k_{cat} - [KS]k_{deg,U}$$

In order to understand the effects of degradation at steady state, note that the total substrate concentration is defined as:

$$[S]_T = [S] + [S^*] + [KS]$$

and the change in total substrate concentration can thus be written:

$$\frac{d[S]_T}{dt} = \frac{d[S]}{dt} + \frac{d[S^*]}{dt} + \frac{d[KS]}{dt}$$

At steady state, $d[S]_T/dt = 0$. By substituting the above ODEs and simplifying, we get:

$$\frac{d[S]_T}{dt} = k_{synth} - ([S] + [KS])k_{deg,U} - [S^*]k_{deg,P} = 0$$

We can then solve for k_{synth}:

$$k_{synth} = ([S] + [KS])k_{deg,U} + [S^*]k_{deg,P}$$

We can substitute this equation into the original differential equation for $[S]$ (equation 1.2):

$$\frac{d[S]}{dt} = [KS]k_- - [K][S]k_+ + [KS]k_{deg,U} + [S^*]k_{deg,P} \tag{1.3}$$

Equation 1.3 is useful for two reasons. For one, there is a positive term in the equation corresponding to the degradation of phosphorylated substrate ($[S^*]k_{deg,P}$). This term reflects the fact that, in order for $[S]_T$ to remain constant at steady state, new, unphosphorylated substrate molecules must be synthesized to replace S^* molecules that are degraded. There is thus an "effective" dephosphorylation rate in this system where S^* molecules are converted to S, which corresponds mathematically to an unsaturateable first-order phosphatase. Secondly, we used equation 1.3 instead of 1.2 in our numerical integration, so $[S]_T = [S]_0$ for all time; in other words, while the concentration of unphosphorylated and phosphorylated substrate might change in our simulations, the total concentration of substrate remains constant. This allows us to control total substrate levels by setting the initial substrate concentration, as we do in our other models. One could of course simulate equation 1.2 with a constant k_{synth} that allows total substrate concentration to vary with time; while such transients might have interesting effects on the system, we leave consideration of those effects to future work.

For purposes of display we used the following rate parameters:

Parameter	Value
k_+	0.001 $\text{nM}^{-1}\text{s}^{-1}$
k_-	0.1 s^{-1}
k_{cat}	0.9 s^{-1}
$k_{deg,U}$	1x10^{-7} - 1x10^{-4} s^{-1}
$k_{deg,P}$	1x10^{-7} - 1x10^{-4} s^{-1}

The ranges of $k_{deg,U}$ and $k_{deg,P}$ were used to vary the degradation rate of the substrate across simulations. The simulations started with the following initial concentrations:

Molecular Species	Initial Concentration
K	0 - 1 nM
S	10 μM
KS	0

The range of K was used to set the value of r_{deg} across simulations.

This model was used to generate Fig. 3*B* and *C* of the main text. In Fig. 3*B* we used $k_{deg,U} = k_{deg,P} = \log 2/t_{1/2}$ for $t_{1/2} = 10$, 31, and 187 hrs. The value of r_{deg} was set between 0 and 2 by changing the initial concentration of K so that $[K] = (r_{deg}[S]_0 k_{deg,P})/k_{cat}$ (where r_{deg} was set to the desired value, see Section 3 for the derivation of r_{deg}), which ends up giving a value between 0-0.186 nM. In Fig. 3*C* we first ran the model to steady state with an initial concentration of K at 0.186 nM ($r_{deg} = 2$). All kinase molecules were then removed from the system, and the simulation continued in order to obtain the time courses shown in Fig. 3*C*.

1.5 2-Kinase/1-Phosphatase Loop with "Ordered" Phosphatase Adaptors

In order to characterize the effectiveness of phosphatase adaptors in insulating pathways from phosphatase crosstalk, we first developed the 2-Kinase/1-Phosphatase Loop with Ordered Phosphatase Adaptors. The set of enzymatic reactions for this model are:

$$K_1 + S_1 \underset{k_{-,K,1}}{\overset{k_{+,K,1}}{\rightleftharpoons}} K_1S_1 \xrightarrow{k_{cat,K,1}} K_1 + S_1^*$$

$$K_2 + S_2 \underset{k_{-,K,2}}{\overset{k_{+,K,2}}{\rightleftharpoons}} K_2S_2 \xrightarrow{k_{cat,K,2}} K_2 + S_2^*$$

$$PA_1 + S_1^* \underset{k_{-,P,1}}{\overset{k_{+,P,1}}{\rightleftharpoons}} PA_1S_1^* \xrightarrow{k_{cat,P,1}} PA_1 + S_1$$

$$PA_2 + S_2^* \underset{k_{-,P,2}}{\overset{k_{+,P,2}}{\rightleftharpoons}} PA_2S_2^* \xrightarrow{k_{cat,P,2}} PA_2 + S_2$$

$$P + A_1 \underset{k_{-,A,1}}{\overset{k_{+,A,1}}{\rightleftharpoons}} PA_1$$

$$P + A_2 \underset{k_{-,A,2}}{\overset{k_{+,A,2}}{\rightleftharpoons}} PA_2$$

where $k_{-,A,i}$ represents the dissociation rate of the phosphatase-adaptor complex and $k_{+,A,i}$ represents the association rate. The reactions that include a phosphatase molecule are diagrammed in the inset of Fig. $4A$ of the main text. The set of ODEs describing the concentration of free enzymes are:

$$\frac{d[K_1]}{dt} = [K_1S_1]k_{-,K,1} + [K_1S_1]k_{cat,K,1} - [K_1][S_1]k_{+,K,1}$$
$$\frac{d[K_2]}{dt} = [K_2S_2]k_{-,K,2} + [K_2S_2]k_{cat,K,2} - [K_2][S_2]k_{+,K,2}$$
$$\frac{d[P]}{dt} = [PA_1]k_{-,A,1} + [PA_2]k_{-,A,2} - [P][A_1]k_{+,A,1} - [P][A_2]k_{+,A,2}$$

The set of ODEs describing the concentration of free unphosphorylated substrates are:

$$\frac{d[S_1]}{dt} = [K_1S_1]k_{-,K,1} + [PA_1S_1^*]k_{cat,P,1} - [K_1][S_1]k_{+,K,1}$$
$$\frac{d[S_2]}{dt} = [K_2S_2]k_{-,K,2} + [PA_2S_2^*]k_{cat,P,2} - [K_2][S_2]k_{+,K,2}$$

The set of ODEs describing the concentration of free phosphorylated substrates are:

$$\frac{d[S_1^*]}{dt} = [PA_1S_1^*]k_{-,P,1} + [K_1S_1]k_{cat,K,1} - [PA_1][S_1^*]k_{+,P,1}$$
$$\frac{d[S_2^*]}{dt} = [PA_2S_2^*]k_{-,P,2} + [K_2S_2]k_{cat,K,2} - [PA_2][S_2^*]k_{+,P,2}$$

The set of ODEs describing the concentration of adaptor-bound phosphatase are:

$$\frac{d[PA_1]}{dt} = [P][A_1]k_{+,A,1} + [PA_1S_1^*]k_{-,P,1} + [PA_1S_1^*]k_{cat,P,1} - [PA_1]k_{-,A,1} - [PA_1][S_1^*]k_{+,P,1}$$
$$\frac{d[PA_2]}{dt} = [P][A_2]k_{+,A,2} + [PA_2S_2^*]k_{-,P,2} + [PA_2S_2^*]k_{cat,P,2} - [PA_2]k_{-,A,2} - [PA_2][S_2^*]k_{+,P,2}$$

The set of ODEs describing the concentration of enzyme-substrate complexes are:

$$\frac{d[K_1S_1]}{dt} = [K_1][S_1]k_{+,K,1} - [K_1S_1]k_{-,K,1} - [K_1S_1]k_{cat,K,1}$$
$$\frac{d[K_2S_2]}{dt} = [K_2][S_2]k_{+,K,2} - [K_2S_2]k_{-,K,2} - [K_2S_2]k_{cat,K,2}$$
$$\frac{d[PA_1S_1^*]}{dt} = [PA_1][S_1^*]k_{+,P,1} - [PA_1S_1^*]k_{-,P,1} - [PA_1S_1^*]k_{cat,P,1}$$
$$\frac{d[PA_2S_2^*]}{dt} = [PA_2][S_2^*]k_{+,P,2} - [PA_2S_2^*]k_{-,P,2} - [PA_2S_2^*]k_{cat,P,2}$$

For purposes of display we used the following rate parameters:

Parameter	Value
$k_{+,K,i}$	0.001 $\text{nM}^{-1}\text{s}^{-1}$
$k_{-,K,i}$	0.1 s^{-1}
$k_{cat,K,i}$	0.9 s^{-1}
$k_{+,P,i}$	0.001 $\text{nM}^{-1}\text{s}^{-1}$
$k_{-,P,i}$	0.1 s^{-1}
$k_{cat,P,i}$	0.9 s^{-1}
$k_{+,A,i}$	0.001 $\text{nM}^{-1}\text{s}^{-1}$
$k_{-,A,i}$	0.1 s^{-1}

where $i = 1$ or 2. Our simulations started with the following initial concentrations:

Molecular Species	Initial Concentration
K_1	0-20 nM
K_2	0-20 nM
P	10 nM
S_1	10 μM
S_2	10 μM
A_1	10^{-1}-10^4 nM
A_2	10^{-1}-10^4 nM

This model is used to generate Fig. 4 of the main text. In Fig. $4A$, r_1 is set to 0.1 by having an initial concentration of K_1 of 1 nM and r_2 is set to 2 by having an initial concentration of K_2 of 20 nM. The initial concentration of the adaptors A_1 and A_2 were then concurrently varied between 10^{-1} to 10^4 nM. In Fig. $4B$, A_1 and A_2 were initialized with total concentration of 10 nM each. The values of r_1 and r_2 were set between 0 and 2 by setting the initial concentrations of K_1 and K_2 between 0 and 20 nM.

1.6 2-Kinase/1-Phosphatase Loop with "Unordered" Phosphatase Adaptors

We also developed a model of a 2-Kinase/1-Phosphatase Loop with Unordered Phosphatase Adaptors. The set of enzymatic reactions for this model are:

$$
\begin{aligned}
K_1 + S_1 &\underset{k_{-,K,1}}{\overset{k_{+,K,1}}{\rightleftharpoons}} K_1S_1 \xrightarrow{k_{cat,K,1}} K_1 + S_1^* \\
K_2 + S_2 &\underset{k_{-,K,2}}{\overset{k_{+,K,2}}{\rightleftharpoons}} K_2S_2 \xrightarrow{k_{cat,K,2}} K_2 + S_2^* \\
PA_1 + S_1^* &\underset{k_{-,P,1}}{\overset{k_{+,P,1}}{\rightleftharpoons}} PA_1S_1^* \\
PA_2 + S_2^* &\underset{k_{-,P,2}}{\overset{k_{+,P,2}}{\rightleftharpoons}} PA_2S_2^* \\
P + A_1S_1^* &\underset{k_{-,A,1}}{\overset{k_{+,A,1}}{\rightleftharpoons}} PA_1S_1^* \\
P + A_2S_2^* &\underset{k_{-,A,2}}{\overset{k_{+,A,2}}{\rightleftharpoons}} PA_2S_2^* \\
PA_1S_1^* &\underset{}{\overset{k_{cat,P,1}}{\rightleftharpoons}} PA_1 + S_1^* \\
PA_2S_2^* &\underset{}{\overset{k_{cat,P,2}}{\rightleftharpoons}} PA_2 + S_2^* \\
P + A_1 &\underset{k_{-,A,1}}{\overset{k_{+,A,1}}{\rightleftharpoons}} PA_1 \\
P + A_2 &\underset{k_{-,A,2}}{\overset{k_{+,A,2}}{\rightleftharpoons}} PA_2 \\
A_1 + S_1^* &\underset{k_{-,P,1}}{\overset{k_{+,P,1}}{\rightleftharpoons}} A_1S_1^* \\
A_2 + S_2^* &\underset{k_{-,P,2}}{\overset{k_{+,P,2}}{\rightleftharpoons}} A_2S_2^*
\end{aligned}
\tag{1.4}
$$

This model differs from the "ordered" model in that the adaptors can first bind the phosphorylated substrate without needing to be bound to a phosphatase catalytic core. These reactions are diagrammed in the inset of Fig. $4A$ of the main text. The set of ODEs describing the concentration of free enzymes are:

$$
\begin{aligned}
\frac{d[K_1]}{dt} &= [K_1S_1]k_{-,K,1} + [K_1S_1]k_{cat,K,1} - [K_1][S_1]k_{+,K,1} \\
\frac{d[K_2]}{dt} &= [K_2S_2]k_{-,K,2} + [K_2S_2]k_{cat,K,2} - [K_2][S_2]k_{+,K,2}
\end{aligned}
$$

$$\frac{d[P]}{dt} = [PA_1]k_{-,A,1} + [PA_2]k_{-,A,2} + [PA_1S_1^*]k_{-,A,1} + [PA_2S_2^*]k_{-,A,2} \\ - [P][A_1]k_{+,A,1} - [P][A_2]k_{+,A,2} - [P][A_1S_1^*]k_{+,A,1} - [P][A_2S_2^*]k_{+,A,2}$$

The set of ODEs describing the concentration of free unphosphorylated substrates are:

$$\frac{d[S_1]}{dt} = [K_1S_1]k_{-,K,1} + [PA_1S_1^*]k_{cat,P,1} - [K_1][S_1]k_{+,K,1}$$
$$\frac{d[S_2]}{dt} = [K_2S_2]k_{-,K,2} + [PA_2S_2^*]k_{cat,P,2} - [K_2][S_2]k_{+,K,2}$$

The set of ODEs describing the concentration of free phosphorylated substrates are:

$$\frac{d[S_1^*]}{dt} = [PA_1S_1^*]k_{-,P,1} + [A_1S_1^*]k_{-,P,1} + [K_1S_1]k_{cat,K,1} - [PA_1][S_1^*]k_{+,P,1} - [A_1][S_1^*]k_{+,P,1}$$
$$\frac{d[S_2^*]}{dt} = [PA_2S_2^*]k_{-,P,2} + [A_2S_2^*]k_{-,P,2} + [K_2S_2]k_{cat,K,2} - [PA_2][S_2^*]k_{+,P,2} - [A_2][S_2^*]k_{+,P,2}$$

The set of ODEs describing the concentration of adaptor-bound phosphatase are:

$$\frac{d[PA_1]}{dt} = [P][A_1]k_{+,A,1} + [PA_1S_1^*]k_{-,P,1} + [PA_1S_1^*]k_{cat,P,1} - [PA_1]k_{-,A,1} - [PA_1][S_1^*]k_{+,P,1}$$
$$\frac{d[PA_2]}{dt} = [P][A_2]k_{+,A,2} + [PA_2S_2^*]k_{-,P,2} + [PA_2S_2^*]k_{cat,P,2} - [PA_2]k_{-,A,2} - [PA_2][S_2^*]k_{+,P,2}$$

The set of ODEs describing the concentration of adaptor-bound phosphorylated substrate are:

$$\frac{d[A_1S_1^*]}{dt} = [A_1][S_1^*]k_{+,P,1} + [PA_1S_1^*]k_{-,A,1} - [A_1S_1^*]k_{-,P,1} - [P][A_1S_1^*]k_{+,A,1}$$
$$\frac{d[A_2S_2^*]}{dt} = [A_2][S_2^*]k_{+,P,2} + [PA_2S_2^*]k_{-,A,2} - [A_2S_2^*]k_{-,P,2} - [P][A_2S_2^*]k_{+,A,2}$$

The set of ODEs describing the concentration of enzyme-substrate complexes are:

$$\frac{d[K_1S_1]}{dt} = [K_1][S_1]k_{+,K,1} - [K_1S_1]k_{-,K,1} - [K_1S_1]k_{cat,K,1}$$
$$\frac{d[K_2S_2]}{dt} = [K_2][S_2]k_{+,K,2} - [K_2S_2]k_{-,K,2} - [K_2S_2]k_{cat,K,2}$$
$$\frac{d[PA_1S_1^*]}{dt} = [PA_1][S_1^*]k_{+,P,1} + [P][A_1S_1^*]k_{+,P,1} - [PA_1S_1^*]k_{-,P,1} - [PA_1S_1^*]k_{-,A,1} - [PA_1S_1^*]k_{cat,P,1}$$
$$\frac{d[PA_2S_2^*]}{dt} = [PA_2][S_2^*]k_{+,P,2} + [P][A_2S_1^*]k_{+,P,2} - [PA_2S_2^*]k_{-,P,2} - [PA_2S_2^*]k_{-,A,2} - [PA_2S_2^*]k_{cat,P,2}$$

For purposes of display we used the following rate parameters:

Parameter	Value
$k_{+,K,i}$	0.001 $\text{nM}^{-1}\text{s}^{-1}$
$k_{-,K,i}$	0.1 s^{-1}
$k_{cat,K,i}$	0.9 s^{-1}
$k_{+,P,i}$	0.001 $\text{nM}^{-1}\text{s}^{-1}$
$k_{-,P,i}$	0.1 s^{-1}
$k_{cat,P,i}$	0.9 s^{-1}
$k_{+,A,i}$	0.001 $\text{nM}^{-1}\text{s}^{-1}$
$k_{-,A,i}$	0.1 s^{-1}

where $i = 1$ or 2. We set the $K_{D,A,i} = k_{-,A,i}/k_{+,A,i} = 100$ nM to represent a reasonably high affinity of the phosphatase catalytic core P with the adaptor domains A_i. We used the same affinity for the binding of the adaptor domain to the substrate. Note that, in this model, the affinity of the phosphatase for the adaptor domain, and the affinity of the adaptor domain for the substrate, does not depend on wether the adaptor is bound to its other partner. Our simulations started with the following initial concentrations:

Molecular Species	Initial Concentration
K_1	0-20 nM
K_2	0-20 nM
P	10 nM
S_1	10 μM
S_2	0-10 μM
A_1	10^{-1}-10^4 nM
A_2	0-10^4 nM

This model is used to generate Fig. 5 of the main text. In Fig. $5A$, r_1 is set to 0.1 by having an initial concentration of K_1 of 1 nM and r_2 is set to 2 by having an initial concentration of K_2 of 20 nM. The initial concentration of the adaptors A_1 and A_2 were then concurrently varied between 10^{-1} to 10^4 nM. In Fig. $5B$, A_1 and A_2 were initialized with total concentration of 10 nM each. The values of r_1 and r_2 were set between 0 and 2 by setting the initial concentration of K_1 and K_2 to between 0 and 20 nM.

2 The responses of the substrates of an unsaturated phosphatase are strictly hyperbolic in r

We have previously shown [1], following the derivation of Goldbeter and Koshland [5], that the change in product concentration S_1^* for an enzyme E with multiple substrates can be defined as:

$$\frac{d[S_1^*]}{dt} = \frac{V_{max,E,1}[S_1]}{\alpha_{E,1}K_{M,E,1} + [S_1]} \tag{2.1}$$

where $\alpha_{E,1} \equiv 1 + \sum_{i \neq 1} \frac{[S_i]}{K_{M,E,i}}$ is an inhibitory constant for substrate competition with S_1 for E. For a futile cycle at steady state we will have $d[S_1^*]/dt = d[S_1]/dt$. For an unsaturated 2K1P loop, $\alpha_{P,i} = 1$ since $K_{M,P,i} \gg [S_i]_0$. Given 2.1, at steady state we have:

$$\frac{V_{max,K,1}[S_1]}{K_{m,K,1} + [S_1]} = \frac{V_{max,P,1}[S_1^*]}{K_{M,P,1} + [S_1^*]} \tag{2.2}$$

Following the standard Michaelis-Menten approach [1, 5], we assume that $[S_i]_0 \gg [K]_0, [P]_0$, giving us $[S_i]_0 = [S_i] + [S_i^*]$, which can be substituted into 2.2:

$$\frac{V_{max,K,1}(1 - S_1^*)}{K_{K,1} + 1 - S_1^*} = \frac{V_{max,P,1}S_1^*}{K_{P,1} + S_1^*} \tag{2.3}$$

where $S_1 \equiv [S_1]/[S_1]_0$, $S_1^* \equiv [S_1^*]/[S_1]_0$, $K_{K,1} \equiv K_{M,K,1}/[S_1]_0$, and $K_{P,1} \equiv K_{M,P,1}/[S_1]_0$. Dividing both sides by $V_{max,P,1}$ we obtain:

$$\frac{r_1(1 - S_1^*)}{K_{K,1} + 1 - S_1^*} = \frac{S_1^*}{K_{P,1} + S_1^*} \tag{2.4}$$

where $r_1 \equiv V_{max,K,1}/V_{max,P,1}$. Since we are assuming the phosphatase to be unsaturated, $K_{P,1} \gg S_1^*$, and as such 2.4 can be simplified to:

$$\frac{r_1(1 - S_1^*)}{K_{K,1} + 1 - S_1^*} = \frac{S_1^*}{K_{P,1}} \tag{2.5}$$

Expanding 2.5, we get:

$$\begin{aligned} r_1K_{P,1} - r_1K_{P,1}S_1^* &= K_{K,1}S_1^* + S_1^* - (S_1^*)^2 \\ (S_1^*)^2 - (1 + K_{K,1} + r_1K_{P,1})S_1^* + r_1K_{P,1} &= 0 \end{aligned} \tag{2.6}$$

Solving for S_1^*, we obtain the expression:

$$S_1^* = \frac{(1 + K_{K,1} + r_1K_{P,1}) - \sqrt{(1 + K_{K,1} + r_1K_{P,1})^2 - 4r_1K_{P,1}}}{2} \tag{2.7}$$

where the negative branch of the quadratic solution is chosen to obtain physically realistic values of S_1^* (i.e. $0 \leq S_1^* \leq 1$). We can show that S_1^* for a 2K1P with an unsaturated phosphatase is strictly hyperbolic in r_1 by taking the second derivative of 2.7 with respect to r_1:

$$\frac{d^2S_1^*}{dr_1^2} = -\frac{2K_{K,1}K_{P,1}^2}{(-4r_1K_{P,1} + (1 + K_{K,1} + r_1K_{P,1})^2)^{3/2}} \tag{2.8}$$

Note that, for positive real values of both the rate constants and the concentrations, both the numerator and denominator in the above equation are positive. The second derivative is thus always negative (i.e. the curvature is concave), and the variation of S_1^* with r_1 lacks an inflection point. As a result, a system with unsaturated phosphatases cannot exhibit the sigmoidal behavior characteristic of an ultrasensitive, switch-like response.

3 Analytical solution for 1-Kinase/1-Substrate Model with Synthesis and Degradation

From the ODEs derived in 1.4, we have at steady state:

$$\frac{d[K]}{dt} = [KS]k_- + [KS]k_{cat} + [KS]k_{deg,U} - [K][S]k_+ = 0 \tag{3.1}$$

$$\frac{d[S]}{dt} = [KS]k_- + k_{synth} - [K][S]k_+ - [S]k_{deg,U} = 0 \tag{3.2}$$

$$\frac{d[S^*]}{dt} = [KS]k_{cat} - [S^*]k_{deg,P} = 0 \tag{3.3}$$

$$\frac{d[KS]}{dt} = [K][S]k_+ - [KS]k_- - [KS]k_{cat} - [KS]k_{deg,U} = 0 \tag{3.4}$$

Additionally, we can define the conservation of mass of the kinase K:

$$[K]_0 = [K] + [KS] \tag{3.5}$$

From 3.4 we can define the concentration of KS as:

$$[KS] = \frac{[K][S]k_+}{k_- + k_{cat} + k_{deg,U}} \tag{3.6}$$

Equation 3.6 can then be substituted into 3.5 to define the concentration of free kinase K:

$$\begin{aligned}
[K]_0 &= [K] + \frac{[K][S]k_+}{k_- + k_{cat} + k_{deg,U}} \\
[K]_0 &= [K]\left(1 + \frac{[S]k_+}{k_- + k_{cat} + k_{deg,U}}\right) \\
[K] &= \frac{[K]_0}{1 + \frac{[S]k_+}{k_- + k_{cat} + k_{deg,U}}}
\end{aligned} \tag{3.7}$$

We can then substitute 3.7 into 3.6 to get:

$$[KS] = \frac{[K]_0[S]}{\frac{k_- + k_{cat} + k_{deg,U}}{k_+} + [S]} \tag{3.8}$$

We can simplify 3.8 by defining:

$$K_{M,deg} \equiv \frac{k_- + k_{cat} + k_{deg,U}}{k_+}$$

where $K_{M,deg}$ is the analogue of the Michaelis-Menten constant for the kinase K, taking into account the effects of substrate degradation. Equation 3.8 then can be written:

$$[KS] = \frac{[K]_0[S]}{K_{M,deg} + [S]} \tag{3.9}$$

From 3.3 we obtain the expression:

$$[KS]k_{cat} = [S^*]k_{deg,P}$$

into which we can substitute 3.9 to get:

$$\frac{[K]_0[S]k_{cat}}{K_{M,deg} + [S]} = [S^*]k_{deg,P} \tag{3.10}$$

We can then multiply both sides of 3.10 by $[S]_0/[S]_0$:

$$\frac{[K]_0 S \cdot k_{cat}}{K_{deg} + S} = S^* k_{deg,P}[S_0]$$

where $S \equiv [S]/[S]_0$, $S^* \equiv [S^*]/[S]_0$, and $K_{deg} \equiv K_{M,deg}/[S]_0$. We can then define $r_{deg} \equiv [K]_0 k_{cat}/[S]_0 k_{deg,P}$, the ratio of the maximum velocity of the kinase to the maximum velocity of phosphorylated substrate degradation, to get:

$$\frac{r_{deg} S}{K_{deg} + S} = S^* \tag{3.11}$$

Following the standard Michaelis-Menten assumptions [1,5], we have $[S]_0 \gg [K]_0$. This gives us $[S]_0 = [S] + [S^*]$, or $1 = S + S^*$, which can be substituted into 3.11:

$$\begin{aligned} \frac{r_{deg}(1 - S^*)}{K_{deg} + 1 - S^*} &= S^* \\ r_{deg} - r_{deg}S^* &= K_{deg}S^* + S^* - (S^*)^2 \\ (S^*)^2 - (1{+}r_{deg} + K_{deg})S^* + r_{deg} &= 0 \end{aligned} \tag{3.12}$$

We can then solve 3.12 for S^*:

$$S^* = \frac{1 + r_{deg} + K_{deg} - \sqrt{(1 + r_{deg} + K_{deg})^2 - 4r_{deg}}}{2} \tag{3.13}$$

where we have again chosen the negative branch of the solution to ensure $0 \leq S_1^* \leq 1$. From this derivation, we can see that degradation has two effects on the fraction of phosphorylated substrate. The degradation rate of unphosphorylated substrate can change the saturation of the kinase K by the substrate through altering the Michaelis-Menten-like constant $K_{M,deg}$, in the same way as altering the dissociation or catalytic rates. Additionally, the degradation rate of phosphorylated substrate can modify the magnitude of the fraction of phosphorylated substrate by changing r_{deg}.

We can show that S^* is strictly hyperbolic in r_{deg} by taking the second derivative of 3.13 with regard to r_{deg}:

$$\frac{d^2 S^*}{dr_{deg}^2} = -\frac{2K_{deg}}{(-4r_{deg} + (1 + r_{deg} + K_{deg})^2)^{3/2}} \tag{3.14}$$

As for the response with an unsaturated phosphatase (equation 2.8), both the numerator and denominator of the above equation are strictly positive, so the second derivative is always negative. A system that relies on degradation to achieve effective dephosphorylation thus has no inflection point in r_{deg} and cannot exhibit a sigmoidal response to signals.

4 UniProt Data

We searched the UniProt database for the number of serine/threonine and tyrosine kinases and phosphatases found in all complete eukaryotic genomes [6]. For each genome, we searched for UniProt for reviewed entries that included the enzyme classification numbers for kinases and phosphatases (see Table 1). We then counted the number of entries for each genome in the search results. In order to prevent genomes with small numbers of reviewed kinases or phosphatases from unduly influencing our results, we ignored genomes with less than 5 phosphatases or 5 kinases for any given residue cass (i.e. serine/threonine or tyrosine). This resulted in 16 genomes for serine/threonine enzymes (See Table 2) and 9 genomes for tyrosine enzymes (See Table 3).

Table 1: Enzyme classification numbers used to search UniProt

Enzyme	E.C. Number
Serine/Threonine Phosphatases	3.1.3.3 / 3.1.3.16
Serine/Threonine Kinases	2.7.11.x
Tyrosine Phosphatases	3.1.3.48
Tyrosine Kinases	2.7.10.x

Table 2: The numbers and ratios of serine/threonine kinases and phosphatases from UniProt used in Figure 1 of the main text.

Species	Serine/Threonine Phosphatases	Serine/Threonine Kinases	Ratio
Arabidopsis thaliana	115	559	0.206
Bos taurus	26	81	0.321
Caenohabditis elegans	15	89	0.169
Danio rerio	14	40	0.350
Dictyostelium discoideum	21	222	0.095
Drosophila melanogaster	22	66	0.333
Gallus gallus	9	36	0.250
Homo sapiens	79	372	0.212
Mus musculus	72	374	0.193
Oryctolagus cuniculus	7	23	0.304
Oryza sativa	94	120	0.783
Pongo abelii	10	37	0.270
Rattus norvegivus	40	188	0.213
Saccharomyces cerevisiae	24	124	0.194
Schizosaccharomyces pombe	20	100	0.200
Xenopus laevis	17	72	0.236

Table 3: The numbers and ratios of tyrosine kinases and phosphatases from UniProt used in Figure 1 of the main text.

Species	Tyrosine Phosphatases	Tyrosine Kinases	Ratio
Arabidopsis thaliana	9	16	0.563
Bos taurus	13	9	1.444
Caenohabditis elegans	12	11	1.091
Drosophila melanogaster	14	21	0.667
Gallus gallus	11	32	0.344
Homo sapiens	87	95	0.916
Mus musculus	81	95	0.853
Rattus norvegivus	39	49	0.796
Xenopus laevis	11	25	0.440

Additionally, we used UniProt to determine the number of phosphoproteins in complete eukaryotic genomes. We searched UniProt for reviewed entries with keyword 'Phosphoprotein'. We then analyzed the search results and computed the number of entries for each of the 16 species from the serine/threonine enzyme results and the 9 species from the tyrosine enzyme results. The phosphatase numbers represent the total number of phosphatases from tables 2 and 3.

Table 4: The numbers and ratios of the total number of phosphatases and substrates from UniProt used in Figure 1 of the main text.

Species	Total Phosphatases	Total Substrates	Ratio
Arabidopsis thaliana	124	1295	10.444
Bos taurus	39	1759	45.103
Caenohabditis elegans	27	89	3.296
Danio rerio	14	195	13.929
Dictyostelium discoideum	21	160	7.619
Drosophila melanogaster	36	833	23.139
Gallus gallus	20	282	14.100
Homo sapiens	166	5924	35.687
Mus musculus	153	5313	34.725
Oryctolagus cuniculus	7	282	40.286
Oryza sativa	94	150	1.596
Pongo abelii	10	819	81.900
Rattus norvegivus	79	2691	34.063
Saccharomyces cerevisiae	24	2425	101.042
Schizosaccharomyces pombe	20	1067	53.350
Xenopus laevis	28	277	9.893

References

1. Rowland MA, Fontana W, Deeds EJ (2012) Crosstalk and competition in signaling networks. Biophysical Journal 103: 2389-98.

2. Lew J, Taylor SS, Adams JA (1997) Identification of a partially rate-determining step in the catalytic mechanism of camp-dependent protein kinase: a transient kinetic study using stopped-flow fluorescence spectroscopy. Biochemistry 36: 6717-24.

3. Grant BD, Adams JA (1996) Pre-steady-state kinetic analysis of camp-dependent protein kinase using rapid quench flow techniques. Biochemistry 35: 2022-9.

4. Qin S, Pang X, Zhou H (2011) Automated prediction of protein association rate constants. Structure 19: 1744-1751.

5. Goldbeter A, Koshland J D E (1981) An amplified sensitivity arising from covalent modification in biological systems. Proceedings of the National Academy of Sciences of the United States of America 78: 6840-4.

6. Consortium TU (2013) Update on activities at the universal protein resource (uniprot) in 2013. Nucleic Acids Research 41: D43-7.